

SOLUTIONS OF THE EQUATIONS OF CHANGE BY THE AVERAGING  
TECHNIQUE

A THESIS SUBMITTED TO  
THE GRADUATE SCHOOL OF NATURAL AND APPLIED SCIENCES  
OF  
MIDDLE EAST TECHNICAL UNIVERSITY

BY  
MERİÇ DALGIÇ

IN PARTIAL FULFILLMENT OF THE REQUIREMENTS  
FOR  
THE DEGREE OF MASTER OF SCIENCE  
IN  
CHEMICAL ENGINEERING

MAY 2008

Approval of the thesis:

**SOLUTIONS OF THE EQUATIONS OF CHANGE BY THE  
AVERAGING TECHNIQUE**

submitted by **MERİÇ DALGIÇ** in partial fulfillment of the requirements for  
the degree of **Master of Science in Chemical Engineering Department,**  
**Middle East Technical University** by,

Prof. Dr. Canan Özgen \_\_\_\_\_  
Dean, Graduate School of **Natural and Applied Sciences**

Prof. Dr. Gürkan Karakaş \_\_\_\_\_  
Head of Department, **Chemical Engineering**

Prof. Dr. İsmail Tosun \_\_\_\_\_  
Supervisor, **Chemical Engineering Dept., METU**

**Examining Committee Members:**

Prof. Dr. Hayrettin Yücel \_\_\_\_\_  
Chemical Engineering Dept., METU

Prof. Dr. İsmail Tosun \_\_\_\_\_  
Chemical Engineering Dept., METU

Prof. Dr. Levent Yılmaz \_\_\_\_\_  
Chemical Engineering Dept., METU

Prof. Dr. Tülay Durusoy \_\_\_\_\_  
Chemical Engineering Dept., Hacettepe University

Assoc. Prof. Dr. Ahmet Eraslan \_\_\_\_\_  
Engineering Sciences Dept., METU

**Date:** 22.05.2008

I hereby declare that all information in this document has been obtained and presented in accordance with academic rules and ethical conduct. I also declare that, as required by these rules and conduct, I have fully cited and referenced all material and results that are not original to this work.

Name, Last name : Meriç DALGIÇ

Signature :

## ABSTRACT

### SOLUTIONS OF THE EQUATIONS OF CHANGE BY THE AVERAGING TECHNIQUE

DALGIÇ, Meriç

M.S., Department of Chemical Engineering

Supervisor: Prof. Dr. İsmail TOSUN

May 2008, 77 pages

Area averaging is one of the techniques used to solve problems encountered in the transport of momentum, heat, and mass. The application of this technique simplifies the mathematical solution of the problem. However, it necessitates expressing the local value of the dependent variable and/or its derivative(s) on the system boundaries in terms of the averaged variable. In this study, these expressions are obtained by the two-point Hermite expansion and this approximate method is applied to some specific problems, such as, unsteady flow in a concentric annulus, unequal cooling of a long slab, unsteady conduction in a cylindrical rod with internal heat generation, diffusion of a solute into a slab from limited volume of a well-mixed solution, convective mass transport between two parallel plates with a wall reaction, convective mass transport in a cylindrical tube with a wall reaction, and unsteady conduction in a two-layer composite slab. Comparison of the analytical and approximate solutions is shown to be in good agreement for a wide range of dimensionless parameters characterizing each system.

*Keywords:* Transport phenomena, area averaging, two-point Hermite expansion.

## ÖZ

### HAL DEĞİŞİM DENKLEMLERİNİN ORTALAMA YÖNTEMİ İLE ÇÖZÜMÜ

DALGIÇ, Meriç

Yüksek Lisans, Kimya Mühendisliği Bölümü

Tez Yöneticisi: Prof. Dr. İsmail TOSUN

Mayıs 2008, 77 sayfa

Momentum, ısı ve madde taşınımalarında karşılaşılan problemlerin çözümünde kullanılan tekniklerden biri olan ortalamasıdır. Bu yöntemin uygulanması problemin matematiksel çözümünü kolaylaştırır. Ancak bu durumda, bağımlı değişkenin ve/veya türevinin sınır değerlerinin ortalaması alınan değişken cinsinden ifadesi gerekir. Söz konusu sınır değerleri, iki noktalı Hermite açılımı ile elde edilmiş ve taşınım olaylarıyla ilgili problemlerin yaklaşık yöntemle çözümü sistematik olarak gösterilmiştir. Bu çalışmada ele alınan problemler şunlardır: eşmerkezli iki boru arasında yatışkın olmayan akış, uzun bir levhanın asimetric olarak soğutulması, içsel ısı üretimli silindirik bir çubukta yatışkın olmayan ısı iletimi, bir kap içerisindeki sıvıdan uzun bir levhaya difüzyon; iki geniş levha arasında konveksiyon ile madde taşınımı, silindirik bir boruda konveksiyon ile madde taşınımı; iki tabakalı kompozit bir levhada yatışık olmayan ısı iletimi. Analitik ve yaklaşık çözümler, sistemi karakterize eden boyutsuz parametreler cinsinden karşılaştırılmış ve sonuçların uyumlu olduğu gözlenmiştir.

*Anahtar Kelimeler:* Taşınım olayları, alan ortalaması, iki noktalı Hermite açılımı.

To  
My Family and Ercan

## ACKNOWLEDGEMENTS

I would like to express my deep and sincere gratitude to my supervisor Prof. Dr. İsmail TOSUN for his invaluable guidance, criticism, and encouragements throughout this research.

I also wish to thank Assoc. Prof. Dr. Ahmet ERASLAN for his help and software support and also Prof. Dr. Ruşen GEÇİT for his invaluable comments in analytical solutions.

Many thanks to my mother Emine, my father Yetkin, and my sister Melda who have been a great source of strength in all matters of life.

This work would not have been possible without the understanding and encouragement of my colleague and friend, Ercan BARAN. I am grateful to him.

I received financial support from The Scientific and Technological Research Council of Turkey (TÜBİTAK) during my M.Sc. study. This assistance is also gratefully acknowledged.

## TABLE OF CONTENTS

ABSTRACT .....	iv
ÖZ .....	v
DEDICATION .....	vi
ACKNOWLEDGEMENTS .....	vii
TABLE OF CONTENTS .....	viii
LIST OF TABLES .....	x
LIST OF FIGURES .....	xii
LIST OF SYMBOLS .....	xiv
CHAPTERS	
1. INTRODUCTION .....	1
2. TWO-POINT HERMITE EXPANSION .....	3
3. APPLICATIONS .....	8
3.1 Unsteady Flow in a Concentric Annulus .....	8
3.1.1 Analytical Solution .....	9
3.1.2 Approximate Solution by Area Averaging .....	13
3.1.3 Comparison of Results .....	14
3.2 Unequal Cooling of a Long Slab .....	16
3.2.1 Analytical Solution .....	17
3.2.2 Approximate Solution by Area Averaging .....	20
3.2.3 Comparison of Results .....	21
3.2.4 Investigation of the Limiting Case for $T_A = T_B$ .....	24
3.3 Unsteady Heat Conduction in a Cylindrical Rod with Internal Heat Generation .....	26



3.3.1 Analytical Solution .....	27
3.3.2 Approximate Solution by Area Averaging .....	30
3.3.3 Comparison of Results .....	31
3.4 Diffusion of a Solute Into a Long Slab From Limited Volume of a Well-Mixed Solution .....	34
3.4.1 Analytical Solution .....	36
3.4.2 Approximate Solution by Area Averaging .....	37
3.4.3 Comparison of Results .....	39
3.5 Convective Mass Transport Between Two Parallel Plates with a Wall Reaction .....	42
3.5.1 Analytical Solution .....	44
3.5.2 Approximate Solution by Area Averaging .....	47
3.5.3 Comparison of Results .....	49
3.6 Convective Mass Transport in a Cylindrical Tube with a Wall Reaction .....	50
3.6.1 Analytical Solution .....	51
3.6.2 Approximate Solution by Area Averaging .....	54
3.6.3 Comparison of Results .....	55
3.7 Unsteady Conduction in a Two-Layer Composite Slab .....	56
3.7.1 Analytical Solution .....	58
3.7.2 Approximate Solution by Area Averaging .....	60
3.7.3 Comparison of Results .....	63
4. CONCLUSIONS .....	66
REFERENCES .....	69
APPENDIX    NUMERICAL RESULTS OF THE SOLUTIONS.....	70

## LIST OF TABLES

### TABLES

Table 2.1	List of Hermite coefficients .....	4
Table 2.2	Two-point Hermite expansions for $\alpha=0$ and $\beta=0$ .....	5
Table 2.3	Two-point Hermite expansions for $\alpha=1$ and $\beta=0$ .....	5
Table 2.4	Two-point Hermite expansions for $\alpha=0$ and $\beta=1$ .....	5
Table 2.5	Two-point Hermite expansions for $\alpha = 1$ and $\beta = 1$ .....	6
Table 2.6	Combination of $\alpha = 1, \beta = 0$ and $\alpha=0, \beta=1$ Hermite expansions .....	6
Table 3.1	The roots of Eq. (3.1.15) for different values of $\kappa$ .....	12
Table 3.2	$\Theta_{exact,\infty}$ and $\Theta_{approx,\infty}$ values under steady conditions .....	16
Table 3.3	The roots of Eq. (3.2.20) as a function of Biot numbers .....	19
Table 3.4	$\tau_\infty$ and $\langle\theta\rangle_\infty$ values as a function of Biot numbers .....	24
Table 3.5	The roots of Eq. (3.3.21) as a function of Biot number .....	29
Table 3.6	$\tau_\infty$ and $\langle\theta\rangle_\infty$ values as a function of Biot number .....	32
Table 3.7	The roots of Eq. (3.4.19) as a function of $\Psi$ .....	37
Table 3.8	The roots of Eq. (3.5.32) as a function of $\Lambda$ .....	47
Table 3.9	The roots of Eq. (3.6.23) as a function of $\Lambda$ .....	53
Table 3.10	The roots of Eq. (3.7.19) for $\gamma= 0.8, \delta=2.5,$ and different Biot numbers .....	59
Table A.1	Numerical results of Eqs. (3.1.28) and (3.1.39) with $\kappa$ as a parameter .....	70
Table A.2	Numerical results of Eqs. (3.1.28) and (3.1.39) with $\kappa$ as a parameter .....	71
Table A.3	Numerical results of Eqs. (3.1.28) and (3.1.39) with $\kappa$ as a parameter .....	71
Table A.4	Numerical results of Eqs. (3.1.28) and (3.1.39) with $\kappa$ as a parameter .....	72
Table A.5	Numerical results of Eqs. (3.2.28) and (3.2.39) with Biot numbers as parameters .....	72

TABLES

Table A.6	Numerical results of Eqs. (3.3.26) and (3.3.34) for Bi = 0.1 with $\Lambda$ as a parameter .....	73
Table A.7	Numerical results of Eqs. (3.3.26) and (3.3.34) for Bi = 1.0 with $\Lambda$ as a parameter .....	73
Table A.8	Numerical results of Eqs. (3.3.26) and (3.3.34) for Bi = 5.0 with $\Lambda$ as a parameter .....	74
Table A.9	Numerical results of Eqs. (3.4.18) and (3.4.32) with $\Psi$ as a parameter .....	74
Table A.10	Numerical results of Eqs. (3.5.37) and (3.5.46) with $\Lambda$ as a parameter .....	75
Table A.11	Numerical results of Eqs. (3.6.29) and (3.6.37) with $\Lambda$ as a parameter .....	75
Table A.12	Numerical results of Eqs. (3.7.28)–(3.7.56) and (3.7.29)–(3.7.57) with Biot numbers as parameters .....	76
Table A.13	Numerical results of Eqs. (3.7.28)–(3.7.56) and (3.7.29)–(3.7.57) with Biot numbers as parameters .....	76
Table A.14	Numerical results of Eqs. (3.7.28)–(3.7.56) and (3.7.29)–(3.7.57) with Biot numbers as parameters .....	76
Table A.15	Numerical results of Eqs. (3.7.28)–(3.7.56) and (3.7.29)–(3.7.57) with Biot numbers as parameters .....	77

## LIST OF FIGURES

### FIGURES

Figure 3.1	Unsteady flow of a Newtonian fluid in a concentric annulus .....	8
Figure 3.2	Comparison of the analytical and approximate results when $0.1 \leq \kappa \leq 0.4$ .....	15
Figure 3.3	Comparison of the analytical and approximate results when $0.5 \leq \kappa \leq 0.8$ .....	15
Figure 3.4	A long slab cooled by convection .....	16
Figure 3.5	Comparison of the analytical and approximate solutions when $\Omega = 1.0, Bi_A = 1.0, Bi_B = 0.1$ .....	22
Figure 3.6	Comparison of the analytical and approximate solutions when $\Omega = 1.0, Bi_A = 5.0, Bi_B = 1.0$ .....	22
Figure 3.7	Comparison of the analytical and approximate solutions when $\Omega = 1.0, Bi_A = 10.0, Bi_B = 1.0$ .....	23
Figure 3.8	Comparison of the analytical and approximate solutions when $\Omega = 0$ with $Bi_A$ and $Bi_B$ as parameters .....	25
Figure 3.9	Comparison of the analytical and approximate solutions when $\Omega = 0, Bi_A = 10.0, Bi_B = 1.0$ .....	26
Figure 3.10	Unsteady conduction in a cylindrical rod with internal heat generation .....	27
Figure 3.11	Comparison of the analytical and approximate solutions when $Bi = 0.1$ with $\Lambda$ as parameter .....	33
Figure 3.12	Comparison of the analytical and approximate solutions when $Bi = 1.0$ with $\Lambda$ as parameter .....	33
Figure 3.13	Comparison of the analytical and approximate solutions when $Bi = 5.0$ with $\Lambda$ as parameter .....	34
Figure 3.14	Diffusion into a long slab from a limited volume .....	34
Figure 3.15	Comparison of the analytical and approximate solutions with $\Psi$ as a parameter .....	39
Figure 3.16	Comparison of the analytical and approximate solutions when $\Psi = 50.0$ .....	40
Figure 3.17	Comparison of the analytical and two approximate solutions when $\Psi = 0.1$ .....	41

FIGURES

Figure 3.18	Comparison of the analytical and two approximate solutions when $\Psi = 10.0$ .....	41
Figure 3.19	Comparison of the analytical and two approximate solutions when $\Psi = 50.0$ .....	42
Figure 3.20	Convective mass transport between two large parallel plates .....	42
Figure 3.21	Comparison of the analytical and approximate solutions with $\Lambda$ as a parameter .....	49
Figure 3.22	Convective mass transport in a cylindrical tube .....	50
Figure 3.23	Comparison of the analytical and approximate solutions with $\Lambda$ as a parameter .....	56
Figure 3.24	Conduction in a two-layer composite slab .....	57
Figure 3.25	Comparison of the analytical and approximate solutions when $Bi_A = 0.5, Bi_B = 1.0$ .....	64
Figure 3.26	Comparison of the analytical and approximate solutions when $Bi_A = 0.5, Bi_B = 5.0$ .....	64
Figure 3.27	Comparison of the analytical and approximate solutions when $Bi_A = 1.0, Bi_B = 5.0$ .....	65
Figure 3.28	Comparison of the analytical and approximate solutions when $Bi_A = 2.0, Bi_B = 5.0$ .....	65

## LIST OF SYMBOLS

$A$	area, $\text{m}^2$
$B$	distance between plates, m
Bi	Biot number
$c$	concentration, $\text{kmol}/\text{m}^3$
$c_b$	bulk concentration, $\text{kmol}/\text{m}^3$
$\widehat{C}_p$	heat capacity at constant pressure, $\text{kJ}/\text{kg} \cdot \text{K}$
$c_s$	solution of concentration in the tank, $\text{kmol}/\text{m}^3$
$c_\infty$	steady-state concentration, $\text{kmol}/\text{m}^3$
$\mathcal{D}$	diffusion coefficient, $\text{m}^2/\text{s}$
$F$	fractional solute uptake
$\mathcal{H}$	partition coefficient
$\langle h \rangle$	average heat transfer coefficient, $\text{W}/\text{m}^2 \cdot \text{K}$
$I$	integral defined by Eq. (2.3)
$k''$	first-order reaction rate constant, $\text{m}/\text{s}$
$L$	thickness of a slab, or pipe length, m
$M$	solute uptake of the slab, $\text{kmol}$
$M_\infty$	maximum solute uptake of the slab, $\text{kmol}$
$P_o$	pipe inlet pressure, Pa
$P_L$	pipe outlet pressure, Pa
$\mathcal{P}$	modified pressure defined by Eq. (3.1.2)
$Q$	volumetric flow rate, $\text{m}^3/\text{s}$
$r$	radial coordinate, m
$R$	pipe radius, m
$\mathfrak{R}$	rate of internal heat generation, $\text{W}/\text{m}^3$
$S_1$	dimensionless term defined by Eq. (3.7.52)
$S_2$	dimensionless term defined by Eq. (3.7.53)
$S_3$	dimensionless term defined by Eq. (3.7.54)
$S_n$	function defined by Eq. (3.2.24), or Eq. (3.5.30)
$T$	temperature, K
$\langle T \rangle$	average temperature, K
$t$	time, s
$V_s$	volume of the solution, $\text{m}^3$
$v_z$	velocity component in the axial direction, $\text{m}/\text{s}$
$W$	plate width, m

$x$	rectangular coordinate, m
$z$	rectangular coordinate, m

*Greek symbols*

$\alpha$	Hermite expansion variable or, thermal diffusivity, $\text{m}^2/\text{s}$
$\beta$	Hermite expansion variable
$\Theta$	dimensionless term defined by Eq. (3.1.27)
$\delta$	ratio of thermal diffusivities of each layer in a composite slab
$\gamma$	ratio of thicknesses of each layer in a composite slab
$\Gamma$	dimensionless term defined by Eq. (3.7.58)
$\kappa$	dimensionless term defined by Eq. (3.7.7) or, ratio of inner and outer radius in an annulus
$\lambda_n$	$n^{\text{th}}$ eigenvalue
$\Lambda$	dimensionless term defined by Eq. (3.3.6) or, Thiele parameter, defined by Eq. (3.5.7)
$\mu$	viscosity, Pa. s
$\eta$	dimensionless axial coordinate
$\omega$	dimensionless term defined by Eq. (3.2.36)
$\phi$	dimensionless velocity
$\Pi_1$	dimensionless function defined by Eq. (3.7.20)
$\Pi_2$	dimensionless function defined by Eq. (3.7.21)
$\Psi$	dimensionless term defined by Eq. (3.4.6)
$\tau$	dimensionless time
$\theta$	dimensionless temperature or concentration
$\theta_b$	dimensionless bulk concentration
$\langle\theta\rangle$	dimensionless average temperature or concentration
$\varphi$	dimensionless term defined by Eq. (3.7.49)
$\xi$	dimensionless distance

# CHAPTER 1

## INTRODUCTION

Relationship between the volumetric flow rate and the pressure drop, as well as the amount of heat and/or mass transferred from one phase to another across the phase interface, are of great importance in transport phenomena. For this purpose, it is necessary to solve the equations of change at the microscopic level to determine velocity, temperature, and concentration profiles as a function of position and time. Since these equations appear as partial differential equations most of the time, the solutions usually require tedious and complex analytical and/or numerical techniques.

In experimental studies, in general, the average values of velocity, temperature, and concentration are measured rather than the local values. Once the theoretical distributions of velocity, temperature, and concentration are obtained, it is necessary to get their average values by integrating these distributions either over the area or the volume of the system to compare the experimental results with the theoretical ones. The practical question to be asked at this stage is "Is it possible to get these average values from the governing equations with appropriate initial and boundary conditions without solving them?"

Integration of the equations of change over the area (or volume) of the system reduces the order of the governing differential equation. However, the resulting simplified equation not only contains the average value of the dependent variable, but also the local value of the dependent variable and/or its gradient(s), both evaluated on the system boundaries. To proceed further, local values of the dependent variable and their gradients must be related to the average values. This task can be accomplished by the use of the Hermite polynomials.

The aim of this study is to develop a systematic procedure for the application of the averaging technique by employing the two-point Hermite expansion to different problems. These cases are unsteady flow in a concentric annulus,



unequal cooling of a long slab, unsteady conduction in a cylindrical rod with internal heat generation, diffusion of a solute into a slab from limited volume of a well-mixed solution, convective mass transport between two parallel plates with a wall reaction, convective mass transport in a cylindrical tube with a wall reaction, and unsteady conduction in a two-layer composite slab. The exact and approximate results are compared for various values of the dimensionless parameter(s) characterizing each system.

## CHAPTER 2

### TWO-POINT HERMITE EXPANSION

Mennig *et al.* [1] used two-point Hermite interpolation formula in order to solve linear initial and boundary value problems. They derived Hermite expansion in two different forms. The first one is in integro-differential form represented by

$$\int_a^b f(x) dx = \sum_{n=0}^{\alpha} C_n(\alpha, \beta) (b-a)^{n+1} \left. \frac{d^n f(x)}{dx^n} \right|_{x=a} + \sum_{n=0}^{\beta} C_n(\beta, \alpha) (-1)^n (b-a)^{n+1} \left. \frac{d^n f(x)}{dx^n} \right|_{x=b} \quad (2.1)$$

which expresses the integral  $\int_a^b f(x) dx$  as a linear combination of  $f(a)$ ,  $f(b)$ , and their derivatives. The second formula is in purely differential form represented by

$$f(x)|_{x=b} - f(x)|_{x=a} = \sum_{n=0}^{\alpha} C_n(\alpha, \beta) (b-a)^{n+1} \left. \frac{d^{n+1} f(x)}{dx^{n+1}} \right|_{x=a} + \sum_{n=0}^{\beta} C_n(\beta, \alpha) (-1)^n (b-a)^{n+1} \left. \frac{d^{n+1} f(x)}{dx^{n+1}} \right|_{x=b} \quad (2.2)$$

The coefficients  $C_n(\alpha, \beta)$  appear in Eqs. (2.1) and (2.2) are called Hermite coefficients and some values of  $C_n(\alpha, \beta)$  given by Mennig *et al.* [1] are listed in Table 2.1.

Using the coefficients  $C_n(\alpha, \beta)$ , approximate expressions representing

$$I = \frac{1}{b-a} \int_a^b f(x) dx \quad (2.3)$$

can be obtained by combining Eqs. (2.1) and (2.2). The results are given in Tables 2.2 – 2.5.

Table 2.1. List of Hermite coefficients [1].

$\alpha$	$\beta$	$C_0(\alpha, \beta)$	$C_1(\alpha, \beta)$	$C_2(\alpha, \beta)$	$C_3(\alpha, \beta)$	$C_4(\alpha, \beta)$
0	0	1/2				
0	1	1/3				
0	2	1/4				
0	3	1/5				
0	4	1/6				
1	0	2/3	1/6			
1	1	2/4	1/12			
1	2	2/5	1/20			
1	3	2/6	1/30			
1	4	2/7	1/42			
2	0	3/4	3/12	1/24		
2	1	3/5	3/20	1/60		
2	2	3/6	3/30	1/120		
2	3	3/7	3/42	1/210		
2	4	3/8	3/56	1/336		
3	0	4/5	6/20	4/60	1/120	
3	1	4/6	6/30	4/120	1/360	
3	2	4/7	6/42	4/210	1/840	
3	3	4/8	6/56	4/336	1/1680	
3	4	4/9	6/72	4/504	1/1024	
4	0	5/6	10/30	10/120	5/360	1/720
4	1	5/7	10/42	10/210	5/840	1/2520
4	2	5/8	10/56	10/336	5/1680	1/6720
4	3	5/9	10/72	10/504	5/3024	1/15120
4	4	5/10	10/90	10/720	5/5040	1/30240

Table 2.2. Two-point Hermite expansions for  $\alpha = 0$  and  $\beta = 0$ .

$$I = \frac{1}{2} [ f(x)|_{x=a} + f(x)|_{x=b} ] \quad (\text{A})$$

$$I = f(x)|_{x=a} + \frac{(b-a)}{4} \left( \frac{df}{dx} \Big|_{x=a} + \frac{df}{dx} \Big|_{x=b} \right) \quad (\text{B})$$

$$I = f(x)|_{x=b} - \frac{(b-a)}{4} \left( \frac{df}{dx} \Big|_{x=a} + \frac{df}{dx} \Big|_{x=b} \right) \quad (\text{C})$$

Table 2.3. Two-point Hermite expansions for  $\alpha = 1$  and  $\beta = 0$ .

$$I = \frac{2}{3} f(x)|_{x=a} + \frac{1}{3} f(x)|_{x=b} + \frac{(b-a)}{6} \frac{df}{dx} \Big|_{x=a} \quad (\text{A})$$

$$I = \frac{5}{12} f(x)|_{x=a} + \frac{7}{12} f(x)|_{x=b} - \frac{(b-a)}{12} \frac{df}{dx} \Big|_{x=b} - \frac{(b-a)^2}{24} \frac{d^2f}{dx^2} \Big|_{x=a} \quad (\text{B})$$

$$I = f(x)|_{x=a} + \frac{7(b-a)}{18} \frac{df}{dx} \Big|_{x=a} + \frac{(b-a)}{9} \frac{df}{dx} \Big|_{x=b} + \frac{(b-a)^2}{18} \frac{d^2f}{dx^2} \Big|_{x=a} \quad (\text{C})$$

$$I = f(x)|_{x=b} - \frac{5(b-a)}{18} \frac{df}{dx} \Big|_{x=a} - \frac{2(b-a)}{9} \frac{df}{dx} \Big|_{x=b} - \frac{(b-a)^2}{9} \frac{d^2f}{dx^2} \Big|_{x=a} \quad (\text{D})$$

Table 2.4. Two-point Hermite expansions for  $\alpha = 0$  and  $\beta = 1$ .

$$I = \frac{1}{3} f(x)|_{x=a} + \frac{2}{3} f(x)|_{x=b} - \frac{(b-a)}{6} \frac{df}{dx} \Big|_{x=b} \quad (\text{A})$$

$$I = \frac{7}{12} f(x)|_{x=a} + \frac{5}{12} f(x)|_{x=b} + \frac{(b-a)}{12} \frac{df}{dx} \Big|_{x=a} - \frac{(b-a)^2}{24} \frac{d^2f}{dx^2} \Big|_{x=b} \quad (\text{B})$$

$$I = f(x)|_{x=a} + \frac{2(b-a)}{9} \frac{df}{dx} \Big|_{x=a} + \frac{5(b-a)}{18} \frac{df}{dx} \Big|_{x=b} - \frac{(b-a)^2}{9} \frac{d^2f}{dx^2} \Big|_{x=b} \quad (\text{C})$$

$$I = f(x)|_{x=b} - \frac{(b-a)}{9} \frac{df}{dx} \Big|_{x=a} - \frac{7(b-a)}{18} \frac{df}{dx} \Big|_{x=b} + \frac{(b-a)^2}{18} \frac{d^2f}{dx^2} \Big|_{x=b} \quad (\text{D})$$

Table 2.5. Two-point Hermite expansions for  $\alpha = 1$  and  $\beta = 1$ .

$$I = \frac{1}{2} f(x)|_{x=a} + \frac{1}{2} f(x)|_{x=b} + \frac{(b-a)}{12} \frac{df}{dx} \Big|_{x=a} - \frac{(b-a)}{12} \frac{df}{dx} \Big|_{x=b} \quad (\text{A})$$

$$I = \frac{1}{3} f(x)|_{x=a} + \frac{2}{3} f(x)|_{x=b} - \frac{(b-a)}{6} \frac{df}{dx} \Big|_{x=b} + \frac{(b-a)^2}{72} \left( \frac{d^2 f}{dx^2} \Big|_{x=b} - \frac{d^2 f}{dx^2} \Big|_{x=a} \right) \quad (\text{B})$$

$$I = \frac{2}{3} f(x)|_{x=a} + \frac{1}{3} f(x)|_{x=b} + \frac{(b-a)}{6} \frac{df}{dx} \Big|_{x=a} + \frac{(b-a)^2}{72} \left( \frac{d^2 f}{dx^2} \Big|_{x=a} - \frac{d^2 f}{dx^2} \Big|_{x=b} \right) \quad (\text{C})$$

$$I = f(x)|_{x=a} + \frac{(b-a)}{3} \frac{df}{dx} \Big|_{x=a} + \frac{(b-a)}{6} \frac{df}{dx} \Big|_{x=b} + \frac{(b-a)^2}{24} \left( \frac{d^2 f}{dx^2} \Big|_{x=a} - \frac{d^2 f}{dx^2} \Big|_{x=b} \right) \quad (\text{D})$$

$$I = f(x)|_{x=b} - \frac{(b-a)}{6} \frac{df}{dx} \Big|_{x=a} - \frac{(b-a)}{3} \frac{df}{dx} \Big|_{x=b} + \frac{(b-a)^2}{24} \left( \frac{d^2 f}{dx^2} \Big|_{x=b} - \frac{d^2 f}{dx^2} \Big|_{x=a} \right) \quad (\text{E})$$

Table 2.6. Combination of  $\alpha = 1, \beta = 0$  and  $\alpha = 0, \beta = 1$  Hermite expansions.

$$f(x)|_{x=a} = 2I - f(x)|_{x=b} - \frac{(b-a)}{6} \frac{df}{dx} \Big|_{x=a} + \frac{(b-a)}{6} \frac{df}{dx} \Big|_{x=b} \quad (\text{A})$$

$$f(x)|_{x=b} = 2I - f(x)|_{x=a} - \frac{(b-a)}{6} \frac{df}{dx} \Big|_{x=a} + \frac{(b-a)}{6} \frac{df}{dx} \Big|_{x=b} \quad (\text{B})$$

$$\frac{df}{dx} \Big|_{x=a} = \frac{12}{(b-a)} I - \frac{6}{(b-a)} f(x)|_{x=a} - \frac{6}{(b-a)} f(x)|_{x=b} + \frac{df}{dx} \Big|_{x=b} \quad (\text{C})$$

$$\frac{df}{dx} \Big|_{x=b} = -\frac{12}{(b-a)} I + \frac{6}{(b-a)} f(x)|_{x=a} + \frac{6}{(b-a)} f(x)|_{x=b} + \frac{df}{dx} \Big|_{x=a} \quad (\text{D})$$

Table 2.6 contains the equations derived from the combination of  $\alpha = 1, \beta = 0$  and  $\alpha = 0, \beta = 1$  Hermite expansions. These equations are employed in most of the problems analyzed in this study.

Özyılmaz [2] applied Hermite expansion in area averaging technique to different engineering problems. He used single Hermite expansion that gave the necessary relationship between the local quantity and the average quantity. In the present case, depending on the problem, combination of more than one Hermite expansion is used. This makes it possible to use higher degree Hermite expansion which increases the accuracy of the averaging technique.

## CHAPTER 3

### APPLICATIONS

In this section, application of the area averaging technique and Hermite expansion to various problems encountered in transport phenomena is presented. The problems analyzed for this purpose are unsteady flow in a concentric annulus, unequal cooling of a long slab, unsteady conduction in a cylindrical rod with internal heat generation, diffusion of a solute into a slab from limited volume of a well-mixed solution, convective mass transport between two parallel plates with a wall reaction, convective mass transport in a cylindrical tube with a wall reaction, and unsteady conduction in a two-layer composite slab. The analytical solutions of these problems are also provided. The analytical and approximate solutions are compared for various dimensionless parameters characterizing each problem.

#### 3.1. Unsteady Flow in a Concentric Annulus

A concentric annulus with inner and outer radii of  $\kappa R$  and  $R$ , respectively, is filled with a stationary incompressible Newtonian fluid as shown in Figure 3.1. At time  $t = 0$ , a constant pressure gradient is imposed and the fluid inside the annulus starts to flow. It is required to determine the volumetric flow rate as a function of time.

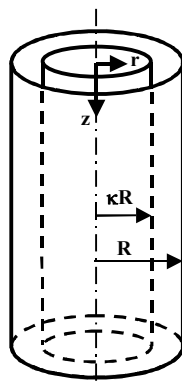


Figure 3.1. Unsteady flow of a Newtonian fluid in a concentric annulus.

Postulating  $v_r = v_\theta = 0$  and  $v_z = v_z(z, t)$ , the  $z$ -component of the equation of motion takes the form

$$\rho \frac{\partial v_z}{\partial t} = \frac{\mathcal{P}_o - \mathcal{P}_L}{L} + \frac{\mu}{r} \frac{\partial}{\partial r} \left( r \frac{\partial v_z}{\partial r} \right) \quad (3.1.1)$$

where  $\mathcal{P}$  is the modified pressure defined by

$$\mathcal{P} = P - \rho g z \quad (3.1.2)$$

The initial and boundary conditions associated with Eq. (3.1.1) are

$$\text{at } t = 0 \quad v_z = 0 \quad (3.1.3)$$

$$\text{at } r = \kappa R \quad v_z = 0 \quad (3.1.4)$$

$$\text{at } r = R \quad v_z = 0 \quad (3.1.5)$$

Introduction of the following dimensionless variables

$$\phi = \frac{v_z}{\frac{(\mathcal{P}_o - \mathcal{P}_L)R^2}{4\mu L}} \quad \xi = \frac{r}{R} \quad \tau = \frac{\mu t}{\rho R^2} \quad (3.1.6)$$

reduces Eqs. (3.1.1) and (3.1.3) – (3.1.5) to the form

$$\frac{\partial \phi}{\partial \tau} = 4 + \frac{1}{\xi} \frac{\partial}{\partial \xi} \left( \xi \frac{\partial \phi}{\partial \xi} \right) \quad (3.1.7)$$

$$\text{at } \tau = 0 \quad \phi = 0 \quad (3.1.8)$$

$$\text{at } \xi = \kappa \quad \phi = 0 \quad (3.1.9)$$

$$\text{at } \xi = 1 \quad \phi = 0 \quad (3.1.10)$$

### 3.1.1. Analytical Solution

Since Eq. (3.1.7) is nonhomogeneous, the solution is proposed in the form

$$\phi(\xi, \tau) = \phi_\infty(\xi) - \phi_t(\xi, \tau) \quad (3.1.11)$$



so that Eq. (3.1.7) is split into two differential equations:  $\phi_\infty(\xi)$  and  $\phi_t(\xi, \tau)$  being the steady-state and transient solutions, respectively. The governing equation and the boundary conditions for  $\phi_\infty(\xi)$  are

$$0 = 4 + \frac{1}{\xi} \frac{d}{d\xi} \left( \xi \frac{d\phi_\infty}{d\xi} \right) \quad (3.1.12)$$

$$\text{at } \xi = \kappa \quad \phi_\infty = 0 \quad (3.1.13)$$

$$\text{at } \xi = 1 \quad \phi_\infty = 0 \quad (3.1.14)$$

The solution of Eq. (3.1.12) is

$$\phi_\infty(\xi) = 1 - \xi^2 - \frac{1 - \kappa^2}{\ln \kappa} \ln \xi \quad (3.1.15)$$

On the other hand, the governing equation for the transient contribution is given by

$$\frac{\partial \phi_t}{\partial \tau} = \frac{1}{\xi} \frac{\partial}{\partial \xi} \left( \xi \frac{\partial \phi_t}{\partial \xi} \right) \quad (3.1.16)$$

with the following initial and boundary conditions

$$\text{at } \tau = 0 \quad \phi_t = \phi_\infty \quad (3.1.17)$$

$$\text{at } \xi = \kappa \quad \phi_t = 0 \quad (3.1.18)$$

$$\text{at } \xi = 1 \quad \phi_t = 0 \quad (3.1.19)$$

The solution of Eq. (3.1.16) is given by

$$\phi_t = 8 \sum_{n=1}^{\infty} \frac{1}{\lambda_n^3} \exp(-\lambda_n^2 \tau) \frac{Z_o(\lambda_n \xi)}{Z_1(\lambda_n) + \kappa Z_1(\lambda_n \kappa)} \quad (3.1.20)$$

where the eigenvalues,  $\lambda_n$ , are the roots of

$$Y_o(\lambda_n \kappa) J_o(\lambda_n) = Y_o(\lambda_n) J_o(\lambda_n \kappa) \quad (3.1.21)$$

and  $Z_n(\lambda_n \xi)$  is defined by

$$Z_n(\lambda_n \xi) = \frac{Y_o(\lambda_n \kappa) J_n(\lambda_n \xi) - Y_n(\lambda_n \xi) J_o(\lambda_n \kappa)}{Y_o(\lambda_n \kappa) J_o(\lambda_n \kappa)} \quad (3.1.22)$$

The first ten eigenvalues for various values of radius ratio,  $\kappa$ , are given in Table 3.1.

The complete solution is obtained by the substitution of Eqs. (3.1.15) and (3.1.20) into Eq. (3.1.11). The result is [3]

$$\phi(\xi, \tau) = 1 - \xi^2 - \frac{1 - \kappa^2}{\ln \kappa} \ln \xi - 8 \sum_{n=1}^{\infty} \frac{1}{\lambda_n^3} \exp(-\lambda_n^2 \tau) \frac{Z_o(\lambda_n \xi)}{Z_1(\lambda_n) + Z_1(\lambda_n \kappa)} \quad (3.1.23)$$

The average velocity is defined by

$$\langle v_z \rangle = \frac{\int_{\kappa R}^R v_z r \, dr}{\int_{\kappa R}^R r \, dr} \quad (3.1.24)$$

In terms of the dimensionless quantities, Eq. (3.1.24) takes the form

$$\langle \phi \rangle = \frac{\langle v_z \rangle}{\frac{(\mathcal{P}_o - \mathcal{P}_L) R^2}{4\mu L}} = \frac{2}{1 - \kappa^2} \int_{\kappa}^1 \phi \xi \, d\xi \quad (3.1.25)$$

Multiplication of the average velocity with the cross-sectional area,  $\pi(1 - \kappa^2)R^2$ , gives the volumetric flow rate. Thus, the dimensionless volumetric flow rate,  $\Theta$ , is given by

$$\Theta = \langle \phi \rangle (1 - \kappa^2) = 2 \int_{\kappa}^1 \phi \xi \, d\xi \quad (3.1.26)$$

where

$$\Theta = \frac{Q}{\pi R^4 (\mathcal{P}_o - \mathcal{P}_L) / 4\mu L} \quad (3.1.27)$$

Substitution of Eq. (3.1.23) into Eq. (3.1.26) and integration give

$$\Theta_{exact} = \frac{1}{2} \left[ 1 - \kappa^4 + \frac{(1 - \kappa^2)^2}{\ln \kappa} \right] - 16 \sum_{n=1}^{\infty} \frac{1}{\lambda_n^4} \left[ \frac{J_o(\lambda_n \kappa) - J_o(\lambda_n)}{J_o(\lambda_n \kappa) + J_o(\lambda_n)} \right] \exp(-\lambda_n^2 \tau) \quad (3.1.28)$$

Table 3.1. The roots of Eq. (3.1.21) for different values of  $\kappa$ .

$n$	$\kappa$							
	0.1	0.2	0.3	0.4	0.5	0.6	0.7	0.8
1	3.314	3.816	4.412	5.183	6.246	7.828	10.455	15.698
2	6.858	7.786	8.933	10.443	12.547	15.695	20.936	31.411
3	10.377	11.732	13.434	15.688	18.836	23.553	31.410	47.121
4	13.886	15.670	17.929	20.929	25.123	31.409	41.884	62.829
5	17.390	19.604	22.422	26.168	31.408	39.265	52.357	78.538
6	20.889	23.536	26.913	31.406	37.706	47.119	62.829	94.246
7	24.387	27.467	31.403	36.643	43.977	54.974	73.301	109.954
8	27.883	31.396	35.892	41.881	50.961	62.829	83.774	125.662
9	31.378	35.326	40.382	47.117	56.544	70.683	94.246	141.371
10	34.872	39.254	44.871	52.354	62.828	78.537	104.718	157.079

### 3.1.2. Approximate Solution by Area Averaging

Area averaging is performed by integrating Eq. (3.1.7) over the cross-sectional flow area, i.e., multiplying Eq. (3.1.7) by  $\xi d\xi$  and integrating from  $\xi = \kappa$  to  $\xi = 1$ . The result is

$$\int_{\kappa}^1 \frac{d\phi}{d\tau} \xi d\xi = 4 \int_{\kappa}^1 \xi d\xi + \int_{\kappa}^1 \frac{\partial}{\partial \xi} \left( \xi \frac{\partial \phi}{\partial \xi} \right) d\xi \quad (3.1.29)$$

or,

$$\frac{d}{d\tau} \int_{\kappa}^1 \phi \xi d\xi = 2(1 - \kappa^2) + \frac{\partial \phi}{\partial \xi} \Big|_{\xi=1} - \kappa \frac{\partial \phi}{\partial \xi} \Big|_{\xi=\kappa} \quad (3.1.30)$$

Substitution of Eq. (3.1.25) into the left-hand side of Eq. (3.1.30) gives

$$\left( \frac{1 - \kappa^2}{2} \right) \frac{d\langle \phi \rangle}{d\tau} = 2(1 - \kappa^2) + \frac{\partial \phi}{\partial \xi} \Big|_{\xi=1} - \kappa \frac{\partial \phi}{\partial \xi} \Big|_{\xi=\kappa} \quad (3.1.31)$$

To proceed further, it is necessary to express  $\partial\phi/\partial\xi|_{\xi=1}$  and  $\partial\phi/\partial\xi|_{\xi=\kappa}$  in terms of the dimensionless average velocity,  $\langle \phi \rangle$ . Hermite expansion for  $\alpha = 1, \beta = 0$ , Eq. (A) in Table 2.3, gives

$$\frac{1}{1 - \kappa} \int_{\kappa}^1 \phi \xi d\xi = \left( \frac{1 + \kappa}{2} \right) \langle \phi \rangle = \frac{2}{3} (\phi \xi)_{\xi=\kappa} + \frac{1}{3} (\phi \xi)_{\xi=1} + \left( \frac{1 - \kappa}{6} \right) \frac{\partial (\xi \phi)}{\partial \xi} \Big|_{\xi=\kappa} \quad (3.1.32)$$

On the other hand, Hermite expansion for  $\alpha = 0, \beta = 1$ , Eq. (A) in Table 2.4, yields

$$\frac{1}{1 - \kappa} \int_{\kappa}^1 \phi \xi d\xi = \left( \frac{1 + \kappa}{2} \right) \langle \phi \rangle = \frac{1}{3} (\phi \xi)_{\xi=\kappa} + \frac{2}{3} (\phi \xi)_{\xi=1} - \left( \frac{1 - \kappa}{6} \right) \frac{\partial (\xi \phi)}{\partial \xi} \Big|_{\xi=1} \quad (3.1.33)$$

Substitution of the boundary conditions defined by Eqs. (3.1.9) and (3.1.10) into Eqs. (3.1.32) and (3.1.33) results in

$$\frac{\partial \phi}{\partial \xi} \Big|_{\xi=\kappa} = \frac{3(1 + \kappa)}{(1 - \kappa)\kappa} \langle \phi \rangle \quad (3.1.34)$$

$$\frac{\partial \phi}{\partial \xi} \Big|_{\xi=1} = -\frac{3(1 + \kappa)}{1 - \kappa} \langle \phi \rangle \quad (3.1.35)$$

The use of Eqs. (3.1.34) and (3.1.35) in Eq. (3.1.31) gives

$$\frac{d\langle\phi\rangle}{d\tau} + \frac{12}{(1-\kappa)^2} \langle\phi\rangle = 4 \quad (3.1.36)$$

The initial condition associated with Eq. (3.1.36) is

$$\text{at } \tau = 0 \quad \langle\phi\rangle = 0 \quad (3.1.37)$$

The solution of Eq. (3.1.36) gives the average dimensionless velocity as

$$\langle\phi\rangle = \frac{(1-\kappa)^2}{3} \left\{ 1 - \exp \left[ -\frac{12\tau}{(1-\kappa)^2} \right] \right\} \quad (3.1.38)$$

Therefore, the dimensionless volumetric flow rate becomes

$$\Theta_{approx} = \frac{(1-\kappa^2)(1-\kappa)^2}{3} \left\{ 1 - \exp \left[ -\frac{12\tau}{(1-\kappa)^2} \right] \right\} \quad (3.1.39)$$

### 3.1.3. Comparison of Results

A comparison of the analytical solution, Eq. (3.1.28), with the approximate one, Eq. (3.1.39), is presented in Figures 3.2 and 3.3 as a function of radius ratio,  $\kappa$ . Numerical values are given in Tables A.1–A.4 in Appendix A. In the calculation of dimensionless volumetric flow rate using Eq. (3.1.28), the first two terms of the series solution are sufficient for convergence of  $\Theta$  when  $\tau \geq 0.04$ . For smaller  $\tau$  values, the third term of the series must also be taken into consideration.

The exact and approximate values almost coincide with each other when  $\kappa \geq 0.5$ . When  $\kappa < 0.5$  and  $\tau \leq 0.4$ , approximate results overestimate the exact ones with the largest deviation of about 13%.

The system reaches steady-state when  $\tau \rightarrow \infty$ . Under these conditions, Eqs. (3.1.28) and (3.1.39) reduce to

$$\Theta_{exact,\infty} = \frac{1}{2} \left[ 1 - \kappa^4 + \frac{(1-\kappa^2)^2}{\ln \kappa} \right] \quad (3.1.40)$$

$$\Theta_{approx,\infty} = \frac{(1-\kappa^2)(1-\kappa)^2}{3} \quad (3.1.41)$$

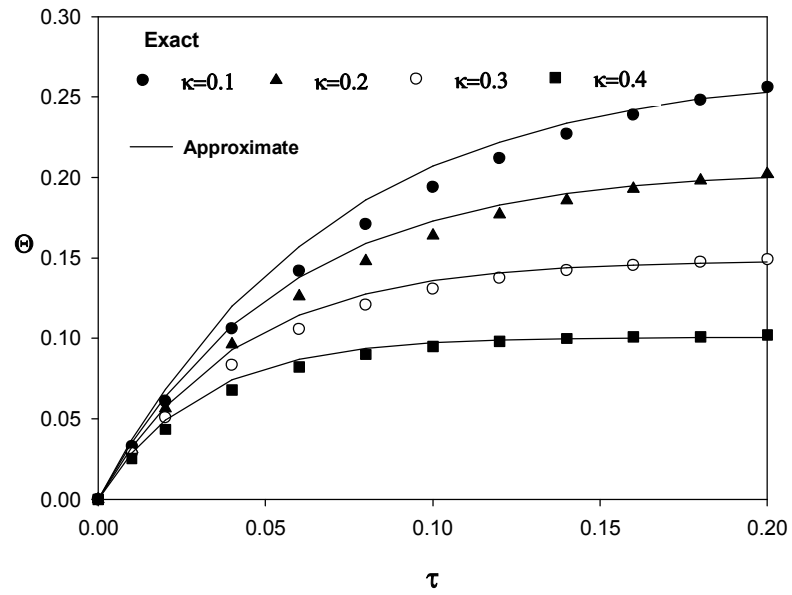


Figure 3.2. Comparison of the analytical and approximate results when  $0.1 \leq \kappa \leq 0.4$ .

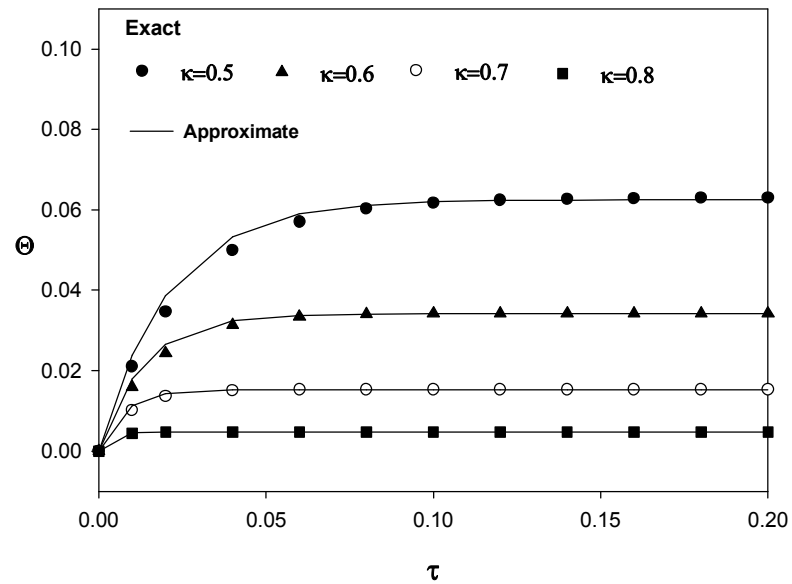


Figure 3.3. Comparison of the analytical and approximate results when  $0.5 \leq \kappa \leq 0.8$ .

From the values given in Table 3.2, the exact and approximate values of the dimensionless volumetric flow rate are almost equal to each other when the radius ratio is greater than 0.3.

Table 3.2.  $\Theta_{exact,\infty}$  and  $\Theta_{approx,\infty}$  values under steady conditions.

$\kappa$	$\Theta_{exact,\infty}$	$\Theta_{approx,\infty}$
0.1	0.287	0.267
0.2	0.213	0.205
0.3	0.152	0.149
0.4	0.102	0.101
0.5	0.063	0.063
0.6	0.034	0.034
0.7	0.015	0.015
0.8	0.0048	0.0048

### 3.2. Unequal Cooling of a Long Slab

A long slab of thickness  $L$ , length  $H$ , and width  $W$  is initially at a uniform temperature of  $T_o$ . At  $t = 0$ , while the surface at  $z = 0$  is exposed to fluid  $A$  at a temperature of  $T_A$ , the surface at  $z = L$  is exposed to fluid  $B$  at a temperature of  $T_B$  ( $T_B < T_A < T_o$ ). The average heat transfer coefficients between the fluids and the surfaces located at  $z = 0$  and  $z = L$  are  $\langle h_A \rangle$  and  $\langle h_B \rangle$ , respectively. The schematic representation of the system is shown in Figure 3.4. It is required to determine the variation of average temperature with time as a result of unequal cooling conditions applied at the surfaces.

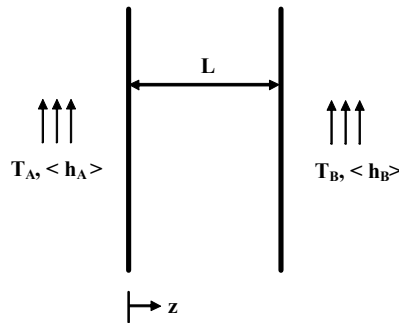


Figure 3.4. A long slab cooled by convection.

When  $L/W \ll 1$  and  $L/H \ll 1$ , the conduction equation takes the form

$$\frac{\partial T}{\partial t} = \alpha \frac{\partial^2 T}{\partial z^2} \quad (3.2.1)$$

with the following initial and boundary conditions

$$\text{at } t = 0 \quad T = T_o \quad (3.2.2)$$

$$\text{at } z = 0 \quad k \frac{\partial T}{\partial z} = \langle h_A \rangle (T - T_A) \quad (3.2.3)$$

$$\text{at } z = L \quad -k \frac{\partial T}{\partial z} = \langle h_B \rangle (T - T_B) \quad (3.2.4)$$

Introduction of the dimensionless variables

$$\begin{aligned} \theta = \frac{T - T_A}{T_o - T_A} \quad \xi = \frac{z}{L} \quad \tau = \frac{\alpha t}{L^2} \quad \text{Bi}_A = \frac{\langle h_A \rangle L}{k} \\ \text{Bi}_B = \frac{\langle h_B \rangle L}{k} \quad \Omega = \text{Bi}_B \left( \frac{T_A - T_B}{T_o - T_A} \right) \end{aligned} \quad (3.2.5)$$

reduces Eqs. (3.2.1) – (3.2.4) to the form

$$\frac{\partial \theta}{\partial \tau} = \frac{\partial^2 \theta}{\partial \xi^2} \quad (3.2.6)$$

$$\text{at } \tau = 0 \quad \theta = 1 \quad (3.2.7)$$

$$\text{at } \xi = 0 \quad \frac{\partial \theta}{\partial \xi} = \text{Bi}_A \theta \quad (3.2.8)$$

$$\text{at } \xi = 1 \quad -\frac{\partial \theta}{\partial \xi} = \text{Bi}_B \theta + \Omega \quad (3.2.9)$$

### 3.2.1. Analytical Solution

Since the boundary condition in Eq. (3.2.9) is nonhomogeneous, the dimensionless temperature distribution is proposed in the form

$$\theta(\xi, \tau) = \theta_\infty(\xi) - \theta_t(\xi, \tau) \quad (3.2.10)$$

so that Eq. (3.2.6) is split into two differential equations:  $\theta_\infty(\xi)$  and  $\theta_t(\xi, \tau)$  being the steady-state and transient solutions, respectively.



The governing equation and the boundary conditions for  $\theta_\infty(\xi)$  are

$$0 = \frac{d^2\theta_\infty}{d\xi^2} \quad (3.2.11)$$

$$\text{at } \xi = 0 \quad \frac{d\theta_\infty}{d\xi} = \text{Bi}_A \theta_\infty \quad (3.2.12)$$

$$\text{at } \xi = 1 \quad -\frac{d\theta_\infty}{d\xi} = \text{Bi}_B \theta_\infty + \Omega \quad (3.2.13)$$

The solution of Eq. (3.2.11) is

$$\theta_\infty(\xi) = -\frac{\Omega(\text{Bi}_A \xi + 1)}{\text{Bi}_B(1 + \text{Bi}_A) + \text{Bi}_A} \quad (3.2.14)$$

On the other hand, the governing equation for the transient contribution is given by

$$\frac{\partial\theta_t}{\partial\tau} = \frac{\partial^2\theta_t}{\partial\xi^2} \quad (3.2.15)$$

with the following initial and boundary conditions

$$\text{at } \tau = 0 \quad \theta_t = \theta_\infty - 1 \quad (3.2.16)$$

$$\text{at } \xi = 0 \quad \frac{\partial\theta_t}{\partial\xi} = \text{Bi}_A \theta_t \quad (3.2.17)$$

$$\text{at } \xi = 1 \quad -\frac{\partial\theta_t}{\partial\xi} = \text{Bi}_B \theta_t \quad (3.2.18)$$

The solution of Eq. (3.2.15) by the method of separation of variables is

$$\theta_t = \sum_{n=1}^{\infty} A_n \left[ \cos(\lambda_n \xi) + \frac{\text{Bi}_A}{\lambda_n} \sin(\lambda_n \xi) \right] \exp(-\lambda_n^2 \tau) \quad (3.2.19)$$

where the eigenvalues,  $\lambda_n$ , are the roots of

$$\tan \lambda_n = \frac{\lambda_n(\text{Bi}_A + \text{Bi}_B)}{\lambda_n^2 - \text{Bi}_A \text{Bi}_B} \quad (3.2.20)$$

The first ten eigenvalues for different Biot numbers are given in Table 3.3.

Table 3.3. The roots of Eq. (3.2.20) as a function of Biot numbers.

$n$	$\text{Bi}_A = 1.0$	$\text{Bi}_A = 5.0$	$\text{Bi}_A = 10.0$
	$\text{Bi}_B = 0.1$	$\text{Bi}_B = 1.0$	$\text{Bi}_B = 1.0$
1	0.9293	1.7523	1.8753
2	3.4523	4.2406	4.5073
3	6.4532	7.0417	7.3549
4	9.5396	9.9888	10.2923
5	12.6528	13.0100	13.2869
6	15.7771	16.0716	16.3189
7	18.9071	19.1570	19.3775
8	22.0404	22.2570	22.4546
9	25.1757	25.3667	25.5445
10	28.3124	28.4831	28.6450

The coefficients  $A_n$  are given by

$$A_n = \frac{2(\text{Bi}_B^2 + \lambda_n^2)}{X_n} [\text{Bi}_A (\cos \lambda_n - 1) - \lambda_n \sin \lambda_n + \Omega S_n] \quad (3.2.21)$$

where

$$Z = \text{Bi}_A + \text{Bi}_B + \text{Bi}_A \text{Bi}_B \quad (3.2.22)$$

$$X_n = \text{Bi}_A \text{Bi}_B Z + (\text{Bi}_A + \text{Bi}_B + \text{Bi}_A^2 + \text{Bi}_B^2) \lambda_n^2 + \lambda_n^4 \quad (3.2.23)$$

$$S_n = \frac{\text{Bi}_A^2 \lambda_n \cos \lambda_n - \sin \lambda_n (\lambda_n^2 \text{Bi}_A + \lambda_n^2 + \text{Bi}_A)}{Z \lambda_n} \quad (3.2.24)$$

The use of Eqs. (3.2.14) and (3.2.19) in Eq. (3.2.10) gives the complete solution as

$$\theta = -\frac{\Omega (\text{Bi}_A \xi + 1)}{Z} - \sum_{n=1}^{\infty} A_n \left[ \cos(\lambda_n \xi) + \frac{\text{Bi}_A}{\lambda_n} \sin(\lambda_n \xi) \right] \exp(-\lambda_n^2 \tau) \quad (3.2.25)$$

The average temperature,  $\langle T \rangle$ , is defined by

$$\langle T \rangle = \frac{1}{L} \int_0^L T dz \quad (3.2.26)$$

In terms of the dimensionless quantities, Eq. (3.2.26) takes the form

$$\langle \theta \rangle = \frac{\langle T \rangle - T_A}{T_o - T_A} = \int_0^1 \theta d\xi \quad (3.2.27)$$

Substitution of Eq. (3.2.25) into Eq. (3.2.27) and integration lead to

$$\langle \theta \rangle_{exact} = -\frac{\Omega (2 + \text{Bi}_A)}{2Z} - \sum_{n=1}^{\infty} \frac{A_n}{\lambda_n} \left[ \sin \lambda_n - \frac{\text{Bi}_A}{\lambda_n} (\cos \lambda_n - 1) \right] \exp(-\lambda_n^2 \tau) \quad (3.2.28)$$

### 3.2.2. Approximate Solution by Area Averaging

Area averaging is performed by integrating Eq. (3.2.6) in the direction of heat flow, i.e.,  $z$ -direction. For this purpose Eq. (3.2.6) is multiplied with  $d\xi$  and integrated from  $\xi = 0$  to  $\xi = 1$ . The result is

$$\int_0^1 \frac{\partial \theta}{\partial \tau} d\xi = \int_0^1 \frac{\partial^2 \theta}{\partial \xi^2} d\xi \quad (3.2.29)$$

or,

$$\frac{d}{d\tau} \int_0^1 \theta d\xi = \left. \frac{\partial \theta}{\partial \xi} \right|_{\xi=1} - \left. \frac{\partial \theta}{\partial \xi} \right|_{\xi=0} \quad (3.2.30)$$

Substitution of Eq. (3.2.27) into the left-hand side, and the boundary conditions defined by Eqs. (3.2.8) and (3.2.9) into the right-hand side of Eq. (3.2.30) give

$$\frac{d \langle \theta \rangle}{d\tau} = - \left( \text{Bi}_B \theta|_{\xi=1} + \text{Bi}_A \theta|_{\xi=0} + \Omega \right) \quad (3.2.31)$$

To proceed further, it is necessary to express  $\theta|_{\xi=1}$  and  $\theta|_{\xi=0}$  in terms of the average temperature,  $\langle \theta \rangle$ . Hermite expansion for  $\alpha = 1$ ,  $\beta = 0$ , Eq. (A) in Table 2.3, gives

$$\int_0^1 \theta d\xi = \langle \theta \rangle = \frac{2}{3} \theta|_{\xi=0} + \frac{1}{3} \theta|_{\xi=1} + \frac{1}{6} \left. \frac{\partial \theta}{\partial \xi} \right|_{\xi=0} \quad (3.2.32)$$

On the other hand, Hermite expansion for  $\alpha = 0$ ,  $\beta = 1$ , Eq. (A) in Table 2.4, yields

$$\int_0^1 \theta d\xi = \langle \theta \rangle = \frac{1}{3} \theta|_{\xi=0} + \frac{2}{3} \theta|_{\xi=1} - \frac{1}{6} \left. \frac{\partial \theta}{\partial \xi} \right|_{\xi=1} \quad (3.2.33)$$

Substitution of the boundary conditions defined by Eqs. (3.2.8) and (3.2.9) into Eqs. (3.2.32) and (3.2.33), respectively, and the simultaneous solution of the resulting equations yield

$$\theta|_{\xi=0} = \frac{6(2 + \text{Bi}_B)}{\omega} \langle \theta \rangle + \frac{2\Omega}{\omega} \quad (3.2.34)$$

$$\theta|_{\xi=1} = \frac{6(2 + \text{Bi}_A)}{\omega} \langle \theta \rangle - \frac{\Omega(4 + \text{Bi}_A)}{\omega} \quad (3.2.35)$$

where

$$\omega = (4 + \text{Bi}_A)(4 + \text{Bi}_B) - 4 \quad (3.2.36)$$

Substitution of Eqs. (3.2.34) and (3.2.35) into Eq. (3.2.31) gives

$$\frac{d\langle \theta \rangle}{d\tau} + \frac{12Z}{\omega} \langle \theta \rangle = -\frac{6(2 + \text{Bi}_A)\Omega}{\omega} \quad (3.2.37)$$

The initial condition associated with Eq. (3.2.37) is

$$\text{at } \tau = 0 \quad \langle \theta \rangle = 1 \quad (3.2.38)$$

Thus, the solution of Eq. (3.2.37) gives the average dimensionless temperature as

$$\langle \theta \rangle_{approx} = -\frac{\Omega(2 + \text{Bi}_A)}{2Z} + \left[ 1 + \frac{\Omega(2 + \text{Bi}_A)}{2Z} \right] \exp\left(-\frac{12Z}{\omega} \tau\right) \quad (3.2.39)$$

### 3.2.3. Comparison of Results

A comparison of the analytical solution, Eq. (3.2.28), with the approximate one, Eq. (3.2.39), for  $\Omega = 1.0$  and different Biot numbers is presented in Figures 3.5 - 3.7. Numerical values are given in Tables A.5 in Appendix A.

The Biot number is the ratio of the heat transfer resistance in the solid phase to the heat transfer resistance in the fluid phase. Thus, when the Biot number is small, temperature variation within the slab is almost uniform. As the Biot number increases, temperature distribution within the slab starts to develop.

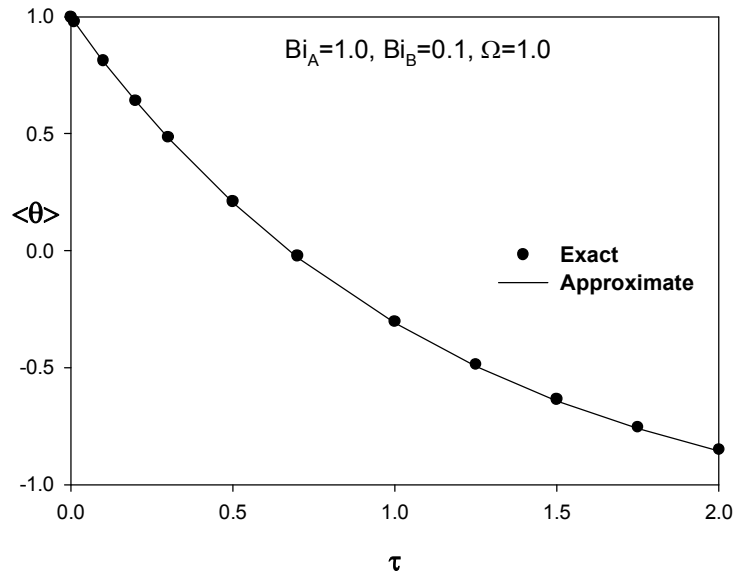


Figure 3.5. Comparison of the analytical and approximate solutions when  $\Omega = 1.0$ ,  $Bi_A = 1.0$ ,  $Bi_B = 0.1$ .

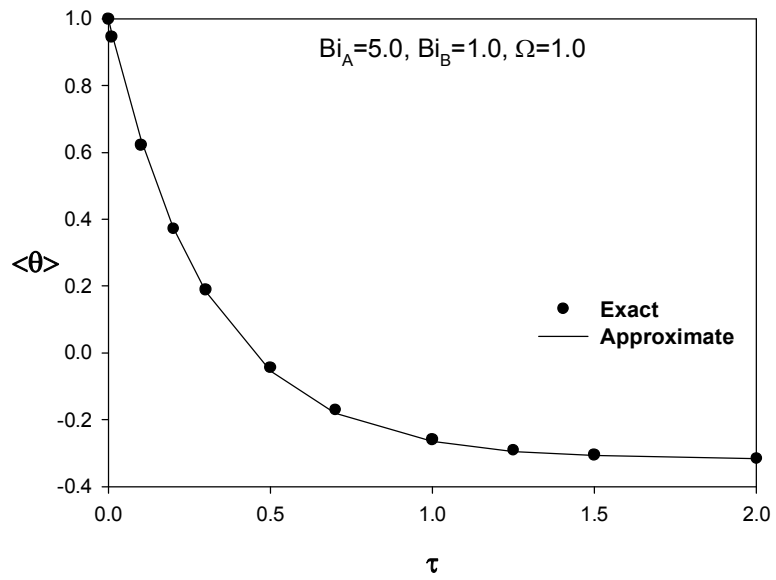


Figure 3.6. Comparison of the analytical and approximate solutions when  $\Omega = 1.0$ ,  $Bi_A = 5.0$ ,  $Bi_B = 1.0$ .

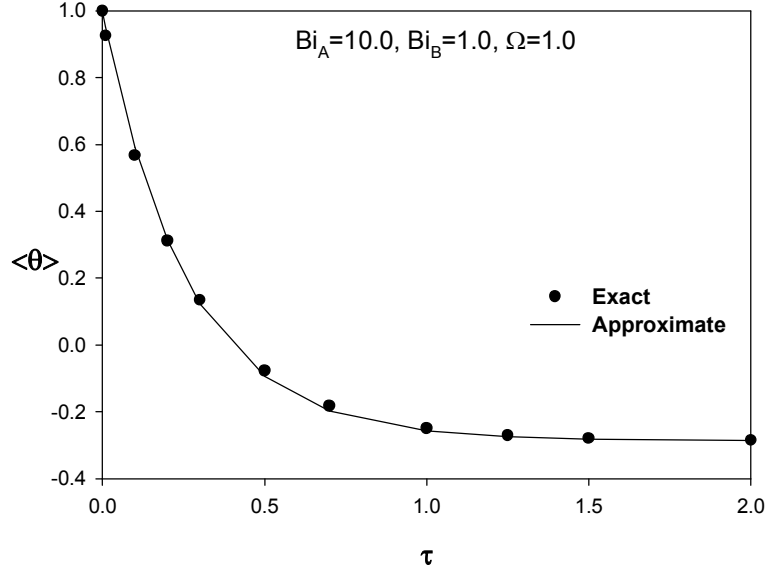


Figure 3.7. Comparison of the analytical and approximate solutions when  $\Omega = 1.0$ ,  $Bi_A = 10.0$ ,  $Bi_B = 1.0$ .

The term  $\Omega$  takes into account the difference between the fluid temperatures,  $T_A$  and  $T_B$ . In the calculation of average temperature using Eq. (3.2.28), the first three terms of the series solution are taken when  $\tau < 0.2$ . When  $\tau \geq 0.2$ , convergence is obtained by considering the first two terms.

Approximate results almost coincide with the exact ones for different values of the Biot numbers, the largest deviation being approximately 8% when  $\tau = 0.3$ ,  $Bi_A = 10.0$ , and  $Bi_B = 1.0$ . An inspection of Figures 3.5 - 3.7 indicates that the dimensionless average temperature,  $\langle\theta\rangle$ , becomes negative as  $\tau$  increases. These negative values result from the definition of  $\langle\theta\rangle$  given by

$$\langle\theta\rangle = \frac{\langle T \rangle - T_A}{T_o - T_A} \quad (3.2.40)$$

Thus,  $\langle\theta\rangle$  takes negative values when  $\langle T \rangle < T_A$ . On the other hand, rearrangement of the  $\Omega$  term defined by Eq. (3.2.5) yields

$$\frac{\Omega}{Bi_B} = \frac{T_A - T_B}{T_o - T_A} \quad (3.2.41)$$

As the temperature difference between the cooling fluids A and B increases, while the numerator of Eq. (3.2.40) becomes more negative, the denominator decreases. As a result,  $\langle\theta\rangle$  values converges to more negative values. Since the values  $\Omega/\text{Bi}_B$  in Figures 3.5 and 3.6 are 10 and 1, respectively,  $\langle\theta\rangle$  values in Figure 3.5 are more negative than the ones in Figure 3.6.

When  $\tau \rightarrow \infty$ , both Eqs. (3.2.28) and (3.2.39) reduce to

$$\langle\theta\rangle_\infty = -\frac{\Omega(2 + \text{Bi}_A)}{2Z} \quad (3.2.42)$$

In other words, the analytical and approximate solutions become identical when the system reaches steady-state. This limiting condition may be used to check the consistency of the approximate solution. The dimensionless time needed to reach steady-state,  $\tau_\infty$ , and the dimensionless average temperature under steady conditions,  $\langle\theta\rangle_\infty$ , are given in Table 3.4. As the Biot number increases, the external (fluid) resistance to heat transfer decreases. As a result, the system reaches steady conditions in a shorter period of time.

Table 3.4.  $\tau_\infty$  and  $\langle\theta\rangle_\infty$  values as a function of Biot numbers.

$\text{Bi}_A$	$\text{Bi}_B$	$\tau_\infty$	$\langle\theta\rangle_\infty$
1.0	0.1	12.3	-1.250
5.0	1.0	2.9	-0.318
10.0	1.0	2.6	-0.286

### 3.2.4. Investigation of the Limiting Case for $T_A = T_B$

When the fluid temperatures are the same, the term  $\Omega$  becomes equal to zero. In this case, Eq. (3.2.28) reduces to

$$\langle\theta\rangle_{exact} = -\sum_{n=1}^{\infty} \frac{A_n^*}{\lambda_n} \left[ \sin \lambda_n - \frac{\text{Bi}_A}{\lambda_n} (\cos \lambda_n - 1) \right] \exp(-\lambda_n^2 \tau) \quad (3.2.43)$$

where

$$A_n^* = \frac{2(\text{Bi}_B^2 + \lambda_n^2)}{S_n} [\text{Bi}_A (\cos \lambda_n - 1) - \lambda_n \sin \lambda_n] \quad (3.2.44)$$

On the other hand, the approximate solution given by Eq. (3.2.39) reduces to

$$\langle \theta \rangle_{approx} = \exp \left( - \frac{12Z}{\omega} \tau \right) \quad (3.2.45)$$

A comparison of the analytical solution, Eq. (3.2.43), with the approximate one, Eq. (3.2.45), for different Biot numbers is given in Figures 3.8 and 3.9. The exact and approximate dimensionless average temperature values almost coincide with each other for all values of the Biot numbers. In this case,  $\langle \theta \rangle$  cannot take negative values since cooling fluid temperatures on both sides of the slab are equal to each other. Su [4] also obtained Eq. (3.2.45) using Hermite expansions for  $\alpha = 0, \beta = 0$  and  $\alpha = 1, \beta = 1$ . However, he compared the approximate results with the ones obtained numerically using the finite difference method.

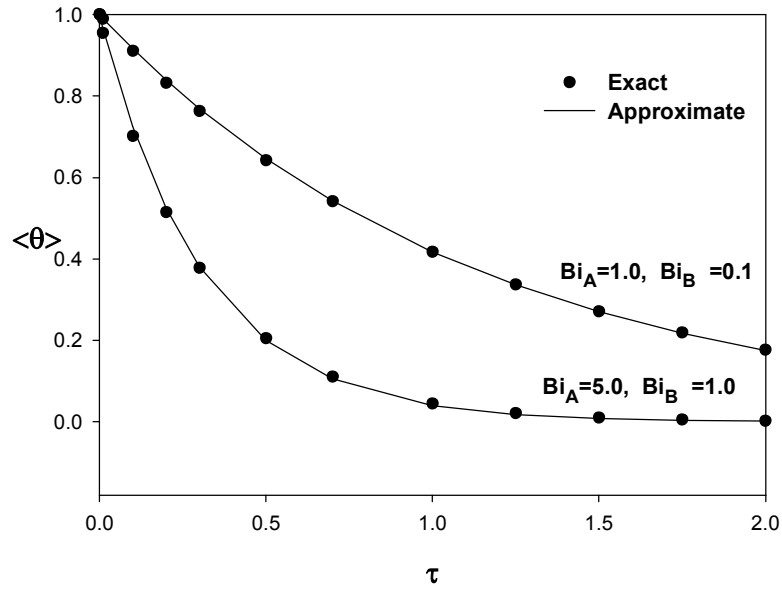


Figure 3.8. Comparison of the analytical and approximate solutions when  $\Omega = 0$  with  $Bi_A$  and  $Bi_B$  as parameters.



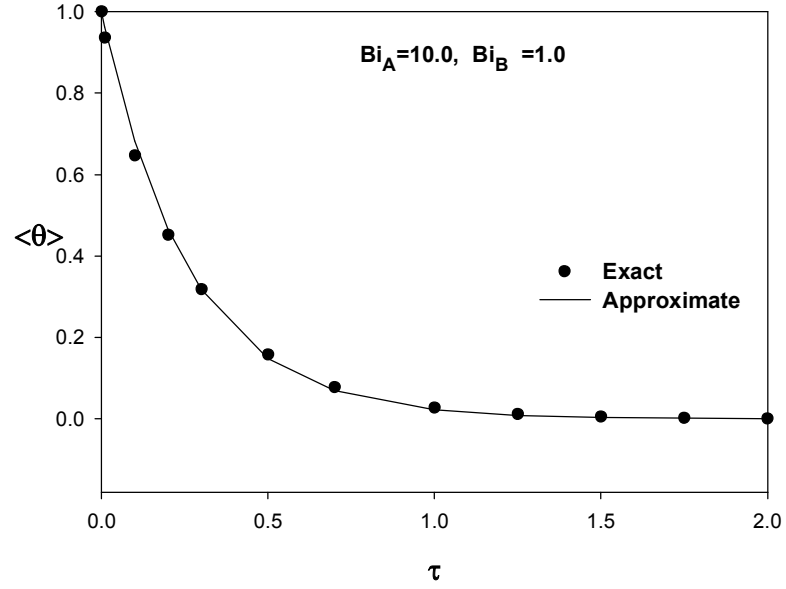


Figure 3.9. Comparison of the analytical and approximate solutions when  $\Omega = 0$ ,  $Bi_A = 10.0$ ,  $Bi_B = 1.0$ .

### 3.3. Unsteady Heat Conduction in a Cylindrical Rod with Internal Heat Generation

A cylindrical rod of radius  $R$ , and length  $L$ , shown in Figure 3.10, is initially at a uniform temperature of  $T_o$ . An internal heat generation starts within the rod at  $t = 0$  with a volumetric rate of

$$\mathfrak{R} = \mathfrak{R}_o r^2 \quad (3.3.1)$$

where  $\mathfrak{R}_o$  is a known constant. The outer surface of the rod is exposed to a cooling fluid at a temperature of  $T_\infty$  ( $T_\infty < T_o$ ) with an average heat transfer coefficient  $\langle h \rangle$ . It is required to find average temperature within the rod as a function of time.

When  $R/L \ll 1$ ,  $r$ -component of the equation of energy takes the form

$$\rho \hat{C}_p \frac{\partial T}{\partial t} = k \frac{\partial}{\partial r} \left( r \frac{\partial T}{\partial r} \right) + \mathfrak{R} \quad (3.3.2)$$

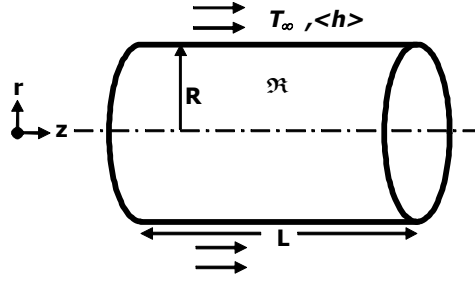


Figure 3.10. Unsteady conduction in a cylindrical rod with internal heat generation.

The initial and boundary conditions associated with Eq. (3.3.2) are

$$\text{at } t = 0 \quad T = T_o \quad (3.3.3)$$

$$\text{at } r = 0 \quad \frac{\partial T}{\partial r} = 0 \quad (3.3.4)$$

$$\text{at } r = R \quad -k \frac{\partial T}{\partial r} = \langle h \rangle (T - T_\infty) \quad (3.3.5)$$

Introduction of the dimensionless variables

$$\theta = \frac{T - T_\infty}{T_o - T_\infty} \quad \xi = \frac{r}{R} \quad \tau = \frac{\alpha t}{R^2} \quad \text{Bi} = \frac{\langle h \rangle R}{k} \quad \Lambda = \left[ \frac{\mathfrak{R}_o R^4}{k (T_o - T_\infty)} \right] \quad (3.3.6)$$

reduces Eqs. (3.3.2) – (3.3.5) to the form

$$\frac{\partial \theta}{\partial \tau} = \frac{1}{\xi} \frac{\partial}{\partial \xi} \left( \xi \frac{\partial \theta}{\partial \xi} \right) + \Lambda \xi^2 \quad (3.3.7)$$

$$\text{at } \tau = 0 \quad \theta = 1 \quad (3.3.8)$$

$$\text{at } \xi = 0 \quad \frac{\partial \theta}{\partial \xi} = 0 \quad (3.3.9)$$

$$\text{at } \xi = 1 \quad -\frac{\partial \theta}{\partial \xi} = \text{Bi} \theta \quad (3.3.10)$$

### 3.3.1. Analytical Solution

Since Eq. (3.3.7) is nonhomogeneous, the solution is proposed in the form

$$\theta(\xi, \tau) = \theta_\infty(\xi) - \theta_t(\xi, \tau) \quad (3.3.11)$$

so that Eq. (3.3.7) is split into two differential equations:  $\theta_\infty(\xi)$  and  $\theta_t(\xi, \tau)$  being the steady-state and transient solutions, respectively. The governing equation and the boundary conditions for  $\theta_\infty(\xi)$  are

$$0 = \frac{1}{\xi} \frac{d}{d\xi} \left( \xi \frac{d\theta_\infty}{d\xi} \right) + \Lambda \xi^2 \quad (3.3.12)$$

$$\text{at } \xi = 0 \quad \frac{d\theta_\infty}{d\xi} = 0 \quad (3.3.13)$$

$$\text{at } \xi = 1 \quad -\frac{d\theta_\infty}{d\xi} = \text{Bi} \theta_\infty \quad (3.3.14)$$

The solution of Eq. (3.3.12) is

$$\theta_\infty = \frac{\Lambda}{16} (1 - \xi^4) + \frac{\Lambda}{4 \text{Bi}} \quad (3.3.15)$$

On the other hand, the governing equation for the transient contribution is given by

$$\frac{\partial \theta_t}{\partial \tau} = \frac{1}{\xi} \frac{\partial}{\partial \xi} \left( \xi \frac{\partial \theta_t}{\partial \xi} \right) \quad (3.3.16)$$

with the following initial and boundary conditions

$$\text{at } \tau = 0 \quad \theta_t = \theta_\infty - 1 \quad (3.3.17)$$

$$\text{at } \xi = 0 \quad \frac{\partial \theta_t}{\partial \xi} = 0 \quad (3.3.18)$$

$$\text{at } \xi = 1 \quad -\frac{\partial \theta_t}{\partial \xi} = \text{Bi} \theta_t \quad (3.3.19)$$

The solution of Eq. (3.3.16) by employing the method of separation of variables is [5]

$$\theta_t = \sum_{n=1}^{\infty} A_n J_0(\lambda_n \xi) \exp(-\lambda_n^2 \tau) \quad (3.3.20)$$

where the eigenvalues,  $\lambda_n$ , are the roots of

$$\lambda_n J_1(\lambda_n) = \text{Bi} J_0(\lambda_n) \quad (3.3.21)$$

The first ten eigenvalues for different Biot numbers are given in Table 3.5.

Table 3.5. The roots of Eq. (3.3.21) as a function of Biot number.

$n$	Bi = 0.1	Bi = 1.0	Bi = 5.0
1	0.4417	1.2558	1.9898
2	3.8577	4.0795	4.7131
3	7.0298	7.1558	7.6177
4	10.1833	10.2710	10.6223
5	13.3312	13.3984	13.6786
6	16.4767	16.5312	16.7630
7	19.6210	19.6667	19.8640
8	22.7645	22.8040	22.9754
9	25.9075	25.9422	26.0937
10	29.0503	29.0812	29.2168

The coefficients  $A_n$  are given by

$$A_n = \frac{\frac{2}{\lambda_n} \left[ \frac{\Lambda}{\lambda_n^2} \left( 1 + \frac{2}{\text{Bi}} - \frac{4}{\lambda_n^2} \right) - 1 \right]}{\left( \frac{\lambda_n^2}{\text{Bi}^2} + 1 \right) J_1(\lambda_n)} \quad (3.3.22)$$

The use of Eqs. (3.3.15) and (3.3.20) in Eq. (3.3.11) gives the complete solution as

$$\theta = \frac{\Lambda}{16} (1 - \xi^4) + \frac{\Lambda}{4\text{Bi}} - \sum_{n=1}^{\infty} A_n J_0(\lambda_n \xi) \exp(-\lambda_n^2 \tau) \quad (3.3.23)$$

The average temperature,  $\langle T \rangle$ , is defined by

$$\langle T \rangle = \frac{\int_0^R T r dr}{\int_0^R r dr} \quad (3.3.24)$$

In terms of the dimensionless quantities, Eq. (3.3.24) takes the form

$$\langle \theta \rangle = \frac{\langle T \rangle - T_\infty}{T_o - T_\infty} = \frac{\int_0^1 \theta \xi d\xi}{\int_0^1 \xi d\xi} = 2 \int_0^1 \theta \xi d\xi \quad (3.3.25)$$

Substitution of Eq. (3.3.23) into Eq. (3.3.25) and integration lead to

$$\langle \theta \rangle_{exact} = \frac{\Lambda (\text{Bi} + 6)}{24 \text{Bi}} - 2 \sum_{n=1}^{\infty} \frac{A_n}{\lambda_n} J_1(\lambda_n) \exp(-\lambda_n^2 \tau) \quad (3.3.26)$$

### 3.3.2. Approximate Solution by Area Averaging

Area averaging is performed by integrating Eq. (3.3.7) over the cross-sectional area of cylinder. For this purpose Eq. (3.3.7) is multiplied by  $\xi d\xi$  and integrated from  $\xi = 0$  to  $\xi = 1$ . The result is

$$\int_0^1 \xi \frac{\partial \theta}{\partial \tau} d\xi = \int_0^1 \frac{\partial}{\partial \xi} \left( \xi \frac{\partial \theta}{\partial \xi} \right) d\xi + \int_0^1 \Lambda \xi^3 d\xi \quad (3.3.27)$$

or,

$$\frac{d}{d\tau} \int_0^1 \theta \xi d\xi = \left( \xi \frac{\partial \theta}{\partial \xi} \right)_{\xi=1} - \left( \xi \frac{\partial \theta}{\partial \xi} \right)_{\xi=0} + \frac{\Lambda}{4} \quad (3.3.28)$$

Substitution of Eq. (3.3.25) into the left-hand side, and the boundary conditions defined by Eqs. (3.3.9) and (3.3.10) into the right-hand side of Eq. (3.3.28) give

$$\frac{d \langle \theta \rangle}{d\tau} = -2 \text{Bi} \theta|_{\xi=1} + \frac{\Lambda}{2} \quad (3.3.29)$$

To proceed further, it is necessary to express  $\theta|_{\xi=1}$  in terms of the average temperature,  $\langle \theta \rangle$ . Hermite expansion for  $\alpha = 1$  and  $\beta = 0$ , Eq. (B) in Table 2.3, yields

$$\int_0^1 \theta \xi d\xi = \frac{1}{2} \langle \theta \rangle = \frac{5}{12} (\theta \xi)_{\xi=0} + \frac{7}{12} (\theta \xi)_{\xi=1} - \frac{1}{12} \frac{\partial (\theta \xi)}{\partial \xi} \Big|_{\xi=1} - \frac{1}{24} \frac{\partial^2 (\theta \xi)}{\partial \xi^2} \Big|_{\xi=0} \quad (3.3.30)$$

The use of the boundary conditions defined by Eqs. (3.3.9) and (3.3.10) into Eq. (3.3.30), and the solution of the resulting equation yield

$$\theta|_{\xi=1} = \left( \frac{6}{6 + \text{Bi}} \right) \langle \theta \rangle \quad (3.3.31)$$

Substitution of Eq. (3.3.31) into Eq. (3.3.29) gives

$$\frac{d \langle \theta \rangle}{d\tau} + \left( \frac{12 \text{Bi}}{6 + \text{Bi}} \right) \langle \theta \rangle = \frac{\Lambda}{2} \quad (3.3.32)$$

The initial condition associated with Eq. (3.3.32) is

$$\text{at } \tau = 0 \quad \langle \theta \rangle = 1 \quad (3.3.33)$$

Thus, the solution of Eq. (3.3.32) gives the average dimensionless temperature as

$$\langle \theta \rangle_{approx} = \frac{\Lambda (\text{Bi} + 6)}{24 \text{Bi}} + \left[ \frac{(24 - \Lambda) \text{Bi} - 6 \Lambda}{24 \text{Bi}} \right] \exp \left( - \frac{12 \text{Bi}}{6 + \text{Bi}} \tau \right) \quad (3.3.34)$$

### 3.3.3. Comparison of Results

A comparison of the analytical solution, Eq. (3.3.26), with the approximate one, Eq. (3.3.34), for different Biot numbers and the dimensionless generation term,  $\Lambda$ , is presented in Figures 3.11 - 3.13. Numerical values are given in Tables A.6–A.8 in Appendix A.

In the calculation of  $\langle \theta \rangle$  using Eq. (3.3.26) the first three terms of the series solution are taken when  $\tau < 0.08$ . For the greater values of  $\tau$ , even the first two terms of the series are sufficient in order to calculate the average temperature.

Even though the rod is exposed to a cooling fluid, the average rod temperature increases with time since the generation term,  $\Lambda$ , dominates the heat loss by convection in all cases. As the Biot number increases, the external resistance to heat transfer decreases, i.e., temperature difference between the rod surface and the cooling fluid decreases. In this case, the temperature difference between the interior and surface temperatures of rod increases with a concomitant increase in heat loss.

The approximate solution gives satisfactory estimates of the dimensionless average temperature for relatively small values of Biot number, i.e.,  $\text{Bi} = 0.1$ , and  $\text{Bi} = 1.0$ . The difference between the analytical and approximate solutions increases as the values of  $\text{Bi}$  and  $\Lambda$  increase. The largest deviation is about 18% when  $\text{Bi} = 5.0$ ,  $\Lambda = 300$ , and  $\tau = 0.2$ .

When  $\tau \rightarrow \infty$ , both Eqs. (3.3.26) and (3.3.34) reduce to

$$\langle \theta \rangle_{\infty} = \frac{\Lambda (\text{Bi} + 6)}{24 \text{Bi}} \quad (3.3.35)$$

In other words, analytical and approximate solutions become identical when the system reaches steady-state. The dimensionless time needed to reach steady-state,  $\tau_\infty$ , and the dimensionless average temperature under steady conditions,  $\langle\theta\rangle_\infty$ , for different Biot numbers are given in Table 3.6.

Table 3.6.  $\tau_\infty$  and  $\langle\theta\rangle_\infty$  values as a function of Biot number.

	Bi = 0.1			Bi = 1.0			Bi = 5.0		
$\Lambda$	50	10	1	100	50	10	300	100	50
$\langle\theta\rangle_\infty$	127.1	25.4	2.5	29.2	14.6	2.9	27.5	9.2	4.6
$\tau_\infty$	84	76	62	10	9	8	4	3.5	3.3

In expressing the physical quantities and/or their derivatives on the system boundaries in terms of the average values, one can use different Hermite expansions. For example, Eq. (3.3.34) is obtained by using Hermite expansion for  $\alpha = 1$ ,  $\beta = 0$ . On the other hand, the use of the Hermite expansion for  $\alpha = 0$ ,  $\beta = 1$ , Eq. (B) in Table 2.4, leads to

$$\langle\theta\rangle_{approx} = \frac{\Lambda (Bi + 3)}{12 Bi} + \left[ \frac{(12 - \Lambda) Bi - 3 \Lambda}{12 Bi} \right] \exp \left( - \frac{6 Bi}{3 + Bi} \tau \right) \quad (3.3.36)$$

In this case, the steady-state solution is given by

$$\langle\theta\rangle_\infty = \frac{\Lambda (Bi + 3)}{12 Bi} \quad (3.3.37)$$

which is different from Eq. (3.3.35). Obtaining identical expressions for the analytical and approximate solutions under steady conditions does not necessarily mean that the Hermite expansion used in the approximate solution is the correct choice; however, the chance of it being correct is fairly high.

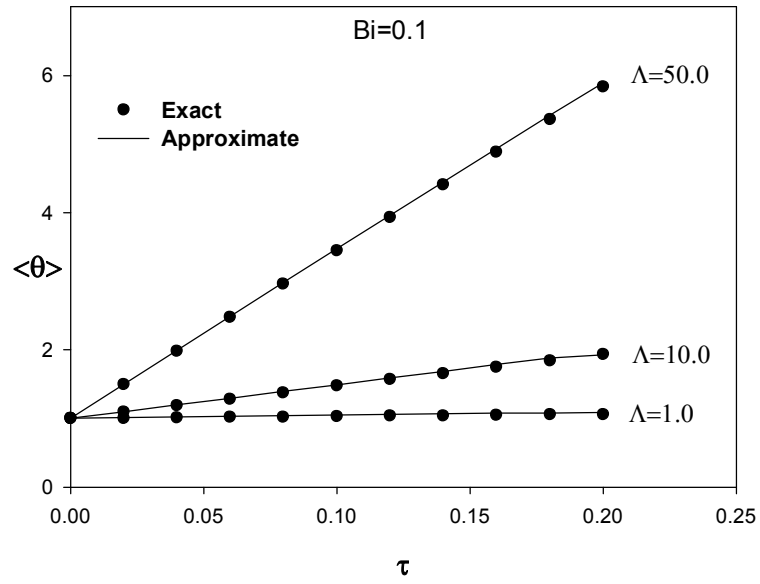


Figure 3.11. Comparison of the analytical and approximate solutions when  $Bi = 0.1$  with  $\Lambda$  as a parameter.

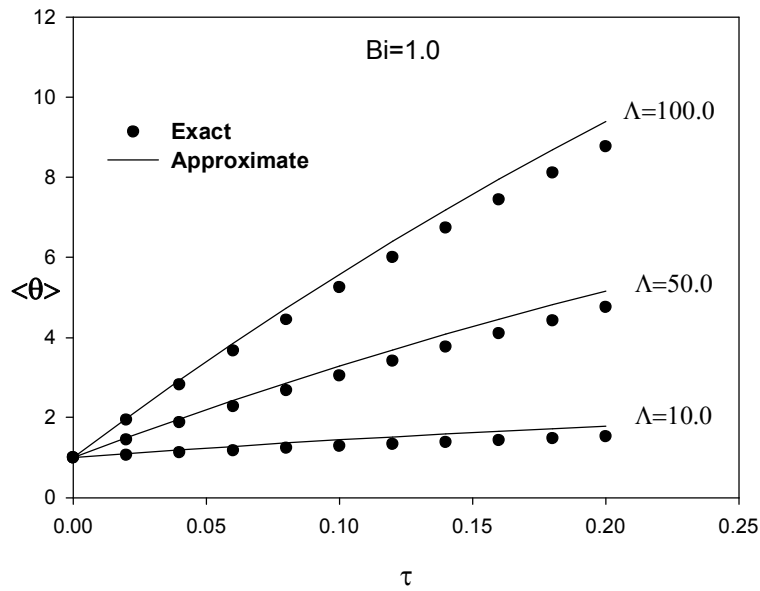


Figure 3.12. Comparison of the analytical and approximate solutions when  $Bi = 1.0$  with  $\Lambda$  as a parameter.



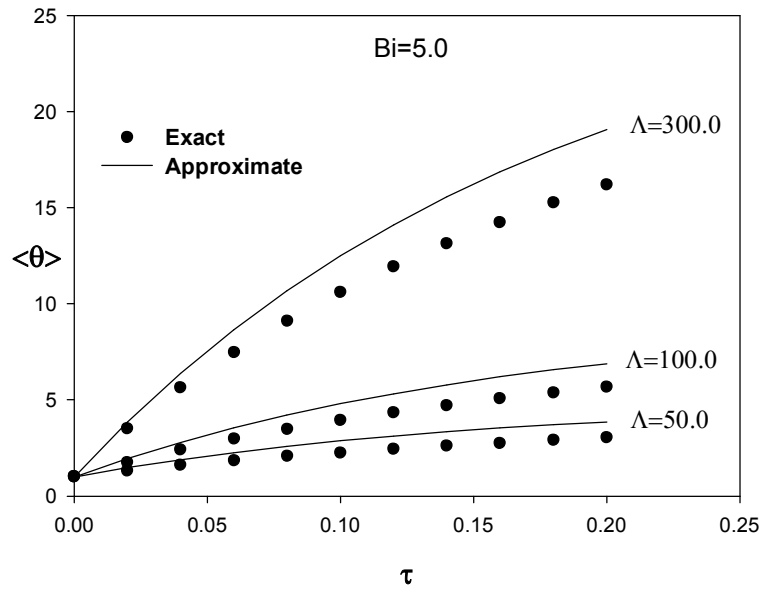


Figure 3.13. Comparison of the analytical and approximate solutions when  $Bi = 5.0$  with  $\Lambda$  as a parameter.

### 3.4. Diffusion of a Solute Into a Long Slab From Limited Volume of a Well-Mixed Solution

A long slab of thickness  $2L$  is suspended in a well-mixed fluid with a limited volume of  $V_s$  as shown in Figure 3.14. While the slab is initially solute-free, the solute concentration in the solution is  $c_{s_0}$ . It is required to obtain an expression relating solute uptake of the slab as a function of time.

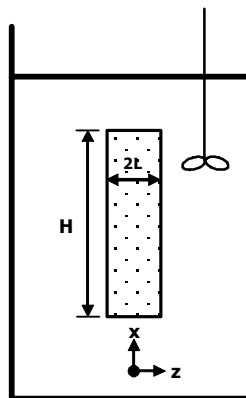


Figure 3.14. Diffusion into a long slab from a limited volume.

Let  $c$  and  $c_s$  be the solute concentrations in the slab and the solution, respectively. When  $L/H \ll 1$ , the governing equations for the slab and the solution take the form

$$\frac{\partial c}{\partial t} = \mathcal{D} \frac{\partial^2 c}{\partial z^2} \quad \text{slab} \quad (3.4.1)$$

$$\left( -\mathcal{D} \frac{\partial c}{\partial z} \Big|_{z=L} \right) 2A = V_s \frac{dc_s}{dt} \quad \text{solution} \quad (3.4.2)$$

where  $A$  is the cross-sectional area of the slab. The initial and boundary conditions are

$$\text{at } t = 0 \quad c = 0 \quad \text{and} \quad c_s = c_{s_0} \quad (3.4.3)$$

$$\text{at } z = 0 \quad \frac{\partial c}{\partial z} = 0 \quad (3.4.4)$$

$$\text{at } z = L \quad c = \mathcal{H} c_s \quad (3.4.5)$$

where  $\mathcal{H}$  is the partition coefficient. Introduction of the following dimensionless variables

$$\theta = \frac{c}{\mathcal{H} c_{s_0}} \quad \theta_s = \frac{c_s}{c_{s_0}} \quad \xi = \frac{z}{L} \quad \tau = \frac{\mathcal{D} t}{L^2} \quad \Psi = \frac{V_s}{2AL\mathcal{H}} \quad (3.4.6)$$

reduces Eqs. (3.4.1) – (3.4.5) to the form

$$\frac{\partial \theta}{\partial \tau} = \frac{\partial^2 \theta}{\partial \xi^2} \quad \text{slab} \quad (3.4.7)$$

$$-\frac{\partial \theta}{\partial \xi} \Big|_{\xi=1} = \Psi \frac{d\theta_s}{d\tau} \quad \text{solution} \quad (3.4.8)$$

$$\text{at } \tau = 0 \quad \theta = 0 \quad \text{and} \quad \theta_s = 1 \quad (3.4.9)$$

$$\text{at } \xi = 0 \quad \frac{\partial \theta}{\partial \xi} = 0 \quad (3.4.10)$$

$$\text{at } \xi = 1 \quad \theta = \theta_s \quad (3.4.11)$$

Once the solute concentration within the slab is determined as a function of position and time, then the solute uptake,  $M$ , is determined from

$$M = 2A \int_0^L c dz \quad (3.4.12)$$

On the other hand, the solute concentration within the slab under steady conditions,  $c_\infty$ , can be determined from a simple macroscopic balance as

$$V_s c_{s_o} = V_s c_\infty + 2AL\mathcal{H}c_\infty \quad (3.4.13)$$

or,

$$c_\infty = \left( \frac{\Psi}{1 + \Psi} \right) c_{s_o} \quad (3.4.14)$$

Therefore, the fractional uptake of the solute,  $F$ , is given by

$$F = \frac{M}{M_\infty} = \frac{2A \int_0^L c dz}{2AL\mathcal{H}c_\infty} = \left( \frac{1 + \Psi}{\Psi} \right) \int_0^1 \theta d\xi \quad (3.4.15)$$

where  $M_\infty$  is the maximum amount of solute transferred into the slab.

Note that Eq. (3.4.15) is also expressed as

$$F = \left( \frac{1 + \Psi}{\Psi} \right) \langle \theta \rangle \quad (3.4.16)$$

where  $\langle \theta \rangle$  represents the average dimensionless concentration defined by

$$\langle \theta \rangle = \frac{\langle c \rangle}{\mathcal{H}c_{s_o}} = \int_0^1 \theta d\xi \quad (3.4.17)$$

### 3.4.1. Analytical Solution

The analytical solution is given by Carslaw and Jaeger [6] as

$$F_{exact} = 1 - 2\Psi(1 + \Psi) \sum_{n=1}^{\infty} \frac{1}{1 + \Psi + (\lambda_n \Psi)^2} \exp(-\lambda_n^2 \tau) \quad (3.4.18)$$

where the eigenvalues,  $\lambda_n$ , are the roots of

$$\tan \lambda_n = -\Psi \lambda_n \quad (3.4.19)$$

The first ten eigenvalues for various values of  $\Psi$  are given in Table 3.7.

Table 3.7. The roots of Eq. (3.4.19) as a function of  $\Psi$ .

$n$	$\Psi = 50.0$	$\Psi = 10.0$	$\Psi = 1.0$
1	1.5834	1.6320	2.0288
2	4.7166	4.7335	4.9132
3	7.8565	7.8667	7.9787
4	10.9974	11.0047	11.0855
5	14.1386	14.1442	14.2074
6	17.2799	17.2845	17.3364
7	20.4213	20.4252	20.4692
8	23.5628	23.5662	23.6043
9	26.7043	26.7073	26.7409
10	29.8458	29.8485	29.8786

### 3.4.2. Approximate Solution by Area Averaging

Area averaging is performed by integrating Eq. (3.4.7) in the direction of mass transfer, i.e.,  $z$ -direction. For this purpose Eq. (3.4.7) is multiplied by  $d\xi$  and integrated from  $\xi = 0$  to  $\xi = 1$ . The result is

$$\int_0^1 \frac{\partial \theta}{\partial \tau} d\xi = \int_0^1 \frac{\partial^2 \theta}{\partial \xi^2} d\xi \quad (3.4.20)$$

or,

$$\frac{d}{d\tau} \int_0^1 \theta d\xi = \left. \frac{\partial \theta}{\partial \xi} \right|_{\xi=1} - \left. \frac{\partial \theta}{\partial \xi} \right|_{\xi=0} \quad (3.4.21)$$

Substitution of Eq. (3.4.17) into the left-hand side, and the boundary condition defined by Eq. (3.4.10) into the right-hand side of Eq. (3.4.21) give

$$\frac{d \langle \theta \rangle}{d\tau} = \left. \frac{\partial \theta}{\partial \xi} \right|_{\xi=1} \quad (3.4.22)$$

Combination of Eqs. (3.4.8) and (3.4.22) gives

$$-\frac{d \langle \theta \rangle}{d\tau} = \Psi \frac{d\theta_s}{d\tau} \quad (3.4.23)$$

The solution of Eq. (3.4.23) using the initial condition of

$$\text{at } \tau = 0 \quad \langle \theta \rangle = 0 \quad \text{and} \quad \theta_s = 1 \quad (3.4.24)$$

leads to

$$\langle \theta \rangle = \Psi(1 - \theta_s) \quad (3.4.25)$$

To proceed one step further, it is necessary to express  $\partial\theta/\partial\xi|_{\xi=1}$  in terms of the dimensionless average concentration,  $\langle \theta \rangle$ . Hermite expansion for  $\alpha = 1, \beta = 0$ , Eq. (A) in Table 2.3, gives

$$\int_0^1 \theta d\xi = \langle \theta \rangle = \frac{2}{3} \theta|_{\xi=0} + \frac{1}{3} \theta|_{\xi=1} + \frac{1}{6} \frac{\partial\theta}{\partial\xi} \Big|_{\xi=0} \quad (3.4.26)$$

On the other hand, Hermite expansion for  $\alpha = 0, \beta = 1$ , Eq. (A) in Table 2.4, yields

$$\int_0^1 \theta d\xi = \langle \theta \rangle = \frac{1}{3} \theta|_{\xi=0} + \frac{2}{3} \theta|_{\xi=1} - \frac{1}{6} \frac{\partial\theta}{\partial\xi} \Big|_{\xi=1} \quad (3.4.27)$$

Substitution of the boundary conditions defined by Eqs. (3.4.10) and (3.4.11) into Eqs. (3.4.26) and (3.4.27), and the simultaneous solutions of the resulting equations yield

$$\frac{\partial\theta}{\partial\xi} \Big|_{\xi=1} = 3(\theta_s - \langle \theta \rangle) \quad (3.4.28)$$

Elimination of  $\theta_s$  between Eqs. (3.4.25) and (3.4.28) results in

$$\frac{\partial\theta}{\partial\xi} \Big|_{\xi=1} = 3 - 3 \left( \frac{1 + \Psi}{\Psi} \right) \langle \theta \rangle \quad (3.4.29)$$

Therefore, the governing equation is obtained by the substitution of Eq. (3.4.29) into Eq. (3.4.22) as

$$\frac{d\langle \theta \rangle}{d\tau} + 3 \left( \frac{1 + \Psi}{\Psi} \right) \langle \theta \rangle = 3 \quad (3.4.30)$$

The solution of Eq. (3.4.30) is

$$\langle \theta \rangle = \frac{\Psi}{1 + \Psi} \left\{ 1 - \exp \left[ -3 \left( \frac{1 + \Psi}{\Psi} \right) \tau \right] \right\} \quad (3.4.31)$$

The use of Eq. (3.4.31) in Eq. (3.4.16) gives the fractional solute uptake as

$$F_{approx} = 1 - \exp \left[ -3 \left( \frac{1 + \Psi}{\Psi} \right) \tau \right] \quad (3.4.32)$$

### 3.4.3. Comparison of Results

A comparison of the analytical solution, Eq. (3.4.18), with the approximate one, Eq. (3.4.32), is presented in Figures 3.15 and 3.16 for various values of  $\Psi$ . Numerical values are given in Table A.9 in Appendix A.

The term  $\Psi$  represents the ratio of the solution volume to the product of the slab volume and the partition coefficient,  $\mathcal{H}$ , relating concentrations of species at the solid-fluid interface under equilibrium conditions [7]. In the calculation of  $F$  using Eq. (3.4.18), the first three terms of the series solution are taken when  $\tau < 0.2$ . For larger values of  $\tau$ , the first two terms are sufficient for convergence.

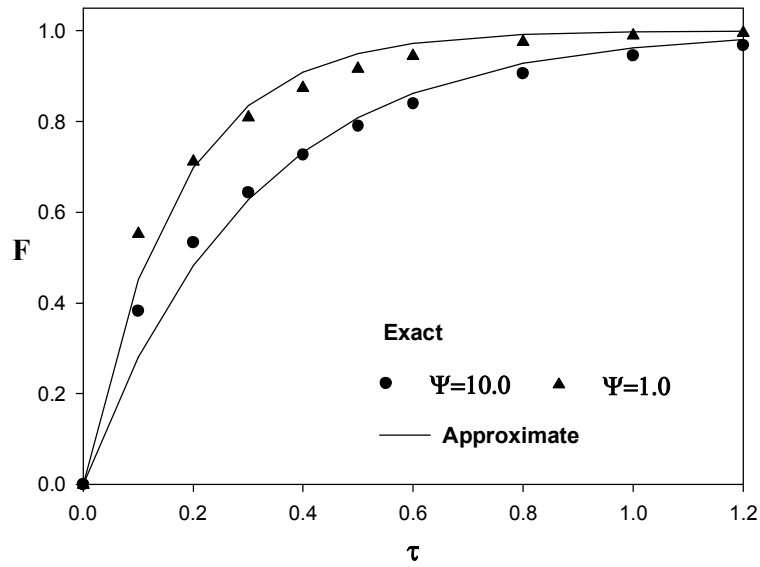


Figure 3.15. Comparison of the analytical and approximate solutions with  $\Psi$  as a parameter.

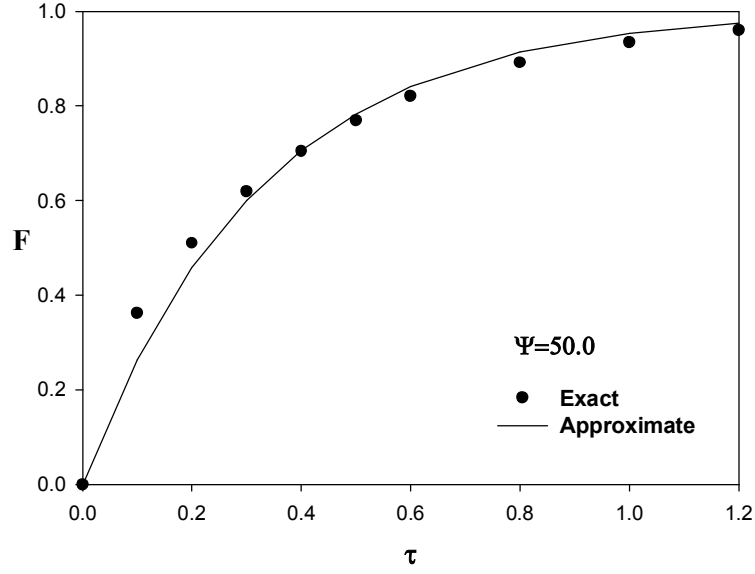


Figure 3.16. Comparison of the analytical and approximate solutions when  $\Psi = 50.0$ .

When  $\Psi \geq 10$ , the exact and approximate results are almost identical for  $\tau \geq 0.3$ . When  $\tau \leq 0.3$ , however, fractional uptake values obtained by the approximate solution underestimates the analytical ones, the largest deviation being 27%.

This problem was also analyzed by Özyılmaz [2] using the Hermite expansion for  $\alpha = 0$  and  $\beta = 0$  approximation. Approximate solution in that case is

$$F_{approx} = 1 - \exp \left[ -4 \left( \frac{1 + \Psi}{\Psi} \right) \tau \right] \quad (3.4.33)$$

A comparison of the analytical solution with the two approximate solutions given by Eqs. (3.4.32) and (3.4.33) for various values of  $\Psi$  is presented in Figures 3.17 – 3.19. The use of  $\alpha = 0$ ,  $\beta = 0$  Hermite expansion gives better estimates of the exact values only for very small values of  $\tau$ , i.e.,  $\tau \leq 0.2$ . When  $\tau > 0.2$ , the combination of  $\alpha = 1$ ,  $\beta = 0$  and  $\alpha = 0$ ,  $\beta = 1$  Hermite expansions improves the results of the approximate technique in a great extent.

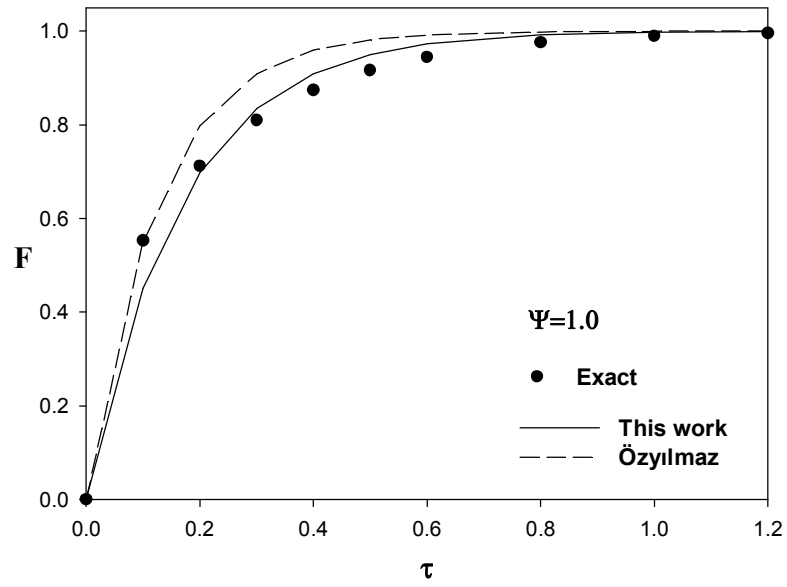


Figure 3.17. Comparison of the analytical and two approximate solutions when  $\Psi = 1.0$ .

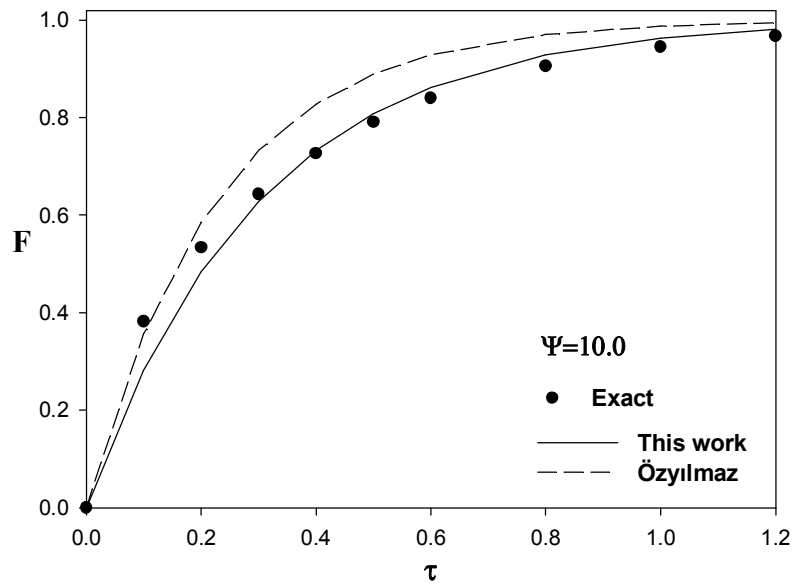


Figure 3.18. Comparison of the analytical and two approximate solutions when  $\Psi = 10.0$ .



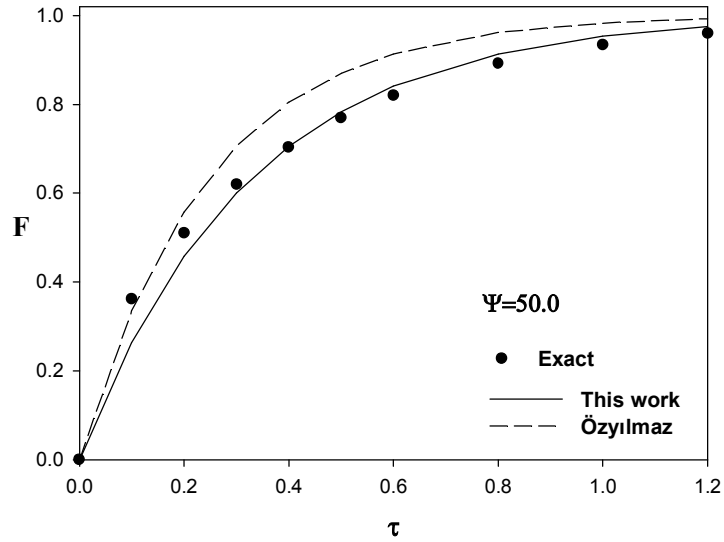


Figure 3.19. Comparison of the analytical and two approximate solutions when  $\Psi = 50.0$ .

### 3.5. Convective Mass Transport with a Wall Reaction Between Two Parallel Plates

An incompressible Newtonian fluid flows between two large parallel plates separated by a distance  $B$  under the action of a constant pressure gradient as shown in Figure 3.20. While a first-order irreversible chemical reaction takes place at the upper plate, the lower plate is impermeable to mass transfer of species. The system is isothermal and it is continuously fed at  $z = 0$  with a dilute solution of chemical reactant with a uniform concentration  $c_0$ . It is required to determine the bulk concentration of species as a function of the axial direction under steady conditions.

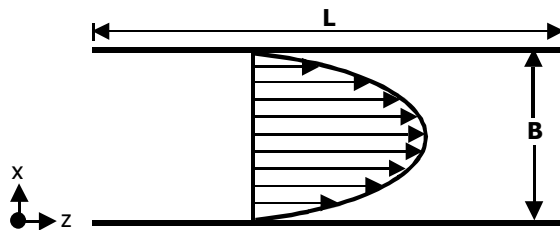


Figure 3.20. Convective mass transport between two large parallel plates.

The fully-developed velocity profile is given by

$$v_z = \frac{(\mathcal{P}_o - \mathcal{P}_L) B^2}{2\mu L} \left[ \frac{x}{B} - \left( \frac{x}{B} \right)^2 \right] \quad (3.5.1)$$

where  $\mathcal{P}$  is the modified pressure defined by

$$\mathcal{P} = P + \rho g x \quad (3.5.2)$$

For large values of Peclet number, the conservation of chemical species under steady conditions takes the form

$$\frac{(\mathcal{P}_o - \mathcal{P}_L) B^2}{2\mu L} \left[ \frac{x}{B} - \left( \frac{x}{B} \right)^2 \right] \frac{\partial c}{\partial z} = \mathcal{D} \frac{\partial^2 c}{\partial x^2} \quad (3.5.3)$$

The boundary conditions associated with Eq. (3.5.3) are

$$\text{at } z = 0 \quad c = c_o \quad (3.5.4)$$

$$\text{at } x = 0 \quad \frac{\partial c}{\partial x} = 0 \quad (3.5.5)$$

$$\text{at } x = B \quad -\mathcal{D} \frac{\partial c}{\partial x} = k'' c \quad (3.5.6)$$

Introduction of the following dimensionless variables

$$\theta = \frac{c}{c_o} \quad \xi = \frac{x}{B} \quad \eta = \frac{2\mu L \mathcal{D} z}{(\mathcal{P}_o - \mathcal{P}_L) B^4} \quad \Lambda = \frac{k'' B}{\mathcal{D}} \quad (3.5.7)$$

reduces Eqs. (3.5.3) – (3.5.6) to the form

$$(\xi - \xi^2) \frac{\partial \theta}{\partial \eta} = \frac{\partial^2 \theta}{\partial \xi^2} \quad (3.5.8)$$

$$\text{at } \eta = 0 \quad \theta = 1 \quad (3.5.9)$$

$$\text{at } \xi = 0 \quad \frac{\partial \theta}{\partial \xi} = 0 \quad (3.5.10)$$

$$\text{at } \xi = 1 \quad -\frac{\partial \theta}{\partial \xi} = \Lambda \theta \quad (3.5.11)$$

### 3.5.1. Analytical Solution

The method of separation of variables is employed in order to solve Eq. (3.5.8). The solution is written in product form as

$$\theta(\xi, \eta) = F(\xi) G(\eta) \quad (3.5.12)$$

so that Eq. (3.5.8) is split into two ordinary differential equations:

$$\frac{dG}{d\eta} + \lambda_n^2 G = 0 \quad (3.5.13)$$

and

$$\frac{1}{\xi - \xi^2} \frac{d^2 F}{d\xi^2} + \lambda_n^2 F = 0 \quad (3.5.14)$$

The solution of Eq. (3.5.13) is

$$G_n(\eta) = \exp(-\lambda_n^2 \eta) \quad (3.5.15)$$

The use of the following transformations

$$X = \frac{\lambda_n}{4} (2\xi - 1)^2 \quad (3.5.16)$$

$$W_n(X) = \frac{F_n}{\sqrt{X}} \exp\left(\frac{X}{2} - \frac{\lambda_n}{8}\right) \quad (3.5.17)$$

reduces Eq. (3.5.14) to

$$X \frac{d^2 W_n}{dX^2} + \left(\frac{3}{2} - X\right) \frac{dW_n}{dX} - \left(\frac{12 - \lambda_n}{16}\right) W_n = 0 \quad (3.5.18)$$

An equation of the type

$$x \frac{d^2 y}{dx^2} + (b - x) \frac{dy}{dx} - ay = 0 \quad (3.5.19)$$

is known as Kummer's equation [8]. One of the solutions of Eq. (3.5.19) is given by

$$y_1 = M(a, b, x) \quad (3.5.20)$$

The term  $M(a, b, x)$  is the Kummer's function of the first kind defined by

$$M(a, b, x) = 1 + \frac{ax}{b} + \frac{(a)_2 x^2}{(b)_2 2!} + \dots + \frac{(a)_n x^n}{(b)_n n!} + \dots \quad (3.5.21)$$

where  $(a)_n$  and  $(b)_n$  are Pochhammer symbols expressed as

$$(\omega)_n = \omega(\omega + 1)(\omega + 2)\dots(\omega + n - 1) \quad \text{with } (\omega)_0 = 1 \quad (3.5.22)$$

Another independent solution of Eq. (3.5.19) is given by

$$y_2 = x^{1-b} M(1 + a - b, 2 - b, x) \quad (3.5.23)$$

Therefore, the solution of Eq. (3.5.19) can be expressed as the sum of solutions, i.e.,

$$y = C_1^* M(a, b, x) + C_2^* x^{1-b} M(1 + a - b, 2 - b, x) \quad (3.5.24)$$

where  $C_1^*$  and  $C_2^*$  are constants. Comparison of Eq. (3.5.18) with Eq. (3.5.19) gives the solution of Eq. (3.5.18) as

$$W_n(X) = C_1^* M\left(\frac{12 - \lambda_n}{16}, \frac{3}{2}, X\right) + \frac{C_2^*}{\sqrt{X}} M\left(\frac{4 - \lambda_n}{16}, \frac{1}{2}, X\right) \quad (3.5.25)$$

Expressing  $X$  in terms of  $\xi$  by using Eq. (3.5.16) reduces Eq. (3.5.24) to the form

$$W_n(\xi) = C_1^* M\left[\frac{12 - \lambda_n}{16}, \frac{3}{2}, \frac{\lambda_n (2\xi - 1)^2}{4}\right] + \frac{C_2^{**}}{2\xi - 1} M\left[\frac{4 - \lambda_n}{16}, \frac{1}{2}, \frac{\lambda_n (2\xi - 1)^2}{4}\right] \quad (3.5.26)$$

where  $C_2^{**}$  is another constant. Finally, substitution of Eq. (3.5.26) into Eq. (3.5.17) leads to the solution as

$$F_n(\xi) = \exp\left[-\frac{\lambda_n}{2}(\xi - 1)\xi\right] \left\{ C_1 (2\xi - 1) M\left[\frac{12 - \lambda_n}{16}, \frac{3}{2}, \frac{\lambda_n (2\xi - 1)^2}{4}\right] + C_2 M\left[\frac{4 - \lambda_n}{16}, \frac{1}{2}, \frac{\lambda_n (2\xi - 1)^2}{4}\right] \right\} \quad (3.5.27)$$

The use of the boundary condition

$$\text{at } \xi = 0 \quad \frac{dF_n}{d\xi} = 0 \quad (3.5.28)$$

gives

$$F_n(\xi) = C_1 \exp \left[ -\frac{\lambda_n}{2} (\xi - 1) \xi \right] \left\{ (2\xi - 1) M \left[ \frac{12 - \lambda_n}{16}, \frac{3}{2}, \frac{\lambda_n (2\xi - 1)^2}{4} \right] + S_n M \left[ \frac{4 - \lambda_n}{16}, \frac{1}{2}, \frac{\lambda_n (2\xi - 1)^2}{4} \right] \right\} \quad (3.5.29)$$

where

$$S_n = \frac{12 (\lambda_n - 4) M \left( \frac{12 - \lambda_n}{16}, \frac{3}{2}, \frac{\lambda_n}{4} \right) + (\lambda_n - 12) \lambda_n M \left( \frac{28 - \lambda_n}{16}, \frac{5}{2}, \frac{\lambda_n}{4} \right)}{3 \lambda_n \left[ 4 M \left( \frac{4 - \lambda_n}{16}, \frac{1}{2}, \frac{\lambda_n}{4} \right) + (\lambda_n - 4) M \left( \frac{20 - \lambda_n}{16}, \frac{3}{2}, \frac{\lambda_n}{4} \right) \right]} \quad (3.5.30)$$

On the other hand, the use of the boundary condition

$$\text{at } \xi = 1 \quad - \frac{dF_n}{d\xi} = \Lambda F_n \quad (3.5.31)$$

gives the following transcendental equation for the eigenvalues  $\lambda_n$

$$12 S_n (\lambda_n - 2\Lambda) M \left( \frac{4 - \lambda_n}{16}, \frac{1}{2}, \frac{\lambda_n}{4} \right) + 12 [\lambda_n - 2(2 + \Lambda)] M \left( \frac{12 - \lambda_n}{16}, \frac{3}{2}, \frac{\lambda_n}{4} \right) = - 3 \lambda_n (\lambda_n - 4) S_n M \left( \frac{20 - \lambda_n}{16}, \frac{3}{2}, \frac{\lambda_n}{4} \right) - \lambda_n (\lambda_n - 12) M \left( \frac{28 - \lambda_n}{16}, \frac{5}{2}, \frac{\lambda_n}{4} \right) \quad (3.5.32)$$

The first ten eigenvalues for various values of  $\Lambda$  are given in Table 3.8. Thus, the complete solution is given by

$$\theta(\xi, \eta) = \sum_{n=1}^{\infty} A_n F_n(\xi) \exp(-\lambda_n^2 \eta) \quad (3.5.33)$$

where the coefficients  $A_n$  are given as

$$A_n = \frac{\int_0^1 F_n(\xi) (\xi - \xi^2) d\xi}{\int_0^1 F_n^2(\xi) (\xi - \xi^2) d\xi} \quad (3.5.34)$$

Table 3.8. The roots of Eq. (3.5.32) as a function of  $\Lambda$ .

$n$	$\Lambda = 0.1$	$\Lambda = 0.5$	$\Lambda = 1.0$
1	0.76055	1.5886	2.0837
2	9.1261	9.3925	9.6706
3	17.1960	17.3740	17.5723
4	25.2269	25.3650	25.5244
5	33.2448	33.3602	33.4952
6	41.2567	41.3568	41.4751
7	49.2653	49.3544	49.4604
8	57.2718	57.3525	57.4489
9	65.2770	65.3510	65.4398
10	73.2812	73.3497	73.4323

The bulk concentration,  $c_b$ , is defined by

$$c_b = \frac{\int_0^W \int_0^B cv_z dx dy}{\int_0^W \int_0^B v_z dx dy} \quad (3.5.35)$$

where  $W$  is the width of the plate. In terms of the dimensionless quantities, Eq. (3.5.35) takes the form

$$\theta_b = \frac{c_b}{c_o} = \frac{\int_0^1 \theta (\xi - \xi^2) d\xi}{\int_0^1 (\xi - \xi^2) d\xi} = 6 \int_0^1 \theta (\xi - \xi^2) d\xi \quad (3.5.36)$$

Substitution of Eq. (3.5.33) into Eq. (3.5.36) and integration give the dimensionless bulk concentration as

$$\theta_{b,exact} = 6 \sum_{n=1}^{\infty} A_n \exp(-\lambda_n^2 \eta) \int_0^1 F_n(\xi) (\xi - \xi^2) d\xi \quad (3.5.37)$$

### 3.5.2. Approximate Solution by Area Averaging

Area averaging is performed by integrating Eq. (3.5.8) over the cross-sectional area of the system. For this purpose Eq. (3.5.8) is multiplied by  $d\xi$  and

integrated from  $\xi = 0$  to  $\xi = 1$ . The result is

$$\int_0^1 (\xi - \xi^2) \frac{\partial \theta}{\partial \eta} d\xi = \int_0^1 \frac{\partial^2 \theta}{\partial \xi^2} d\xi \quad (3.5.38)$$

or,

$$\frac{d}{d\eta} \int_0^1 \theta (\xi - \xi^2) d\xi = \frac{\partial \theta}{\partial \xi} \Big|_{\xi=1} - \frac{\partial \theta}{\partial \xi} \Big|_{\xi=0} \quad (3.5.39)$$

Substitution of Eq. (3.5.36) into the left-hand side, and the boundary conditions defined by Eqs. (3.5.10) and (3.5.11) into the right-hand side of Eq. (3.5.39) give

$$\frac{1}{6} \frac{d\theta_b}{d\eta} = -\Lambda \theta|_{\xi=1} \quad (3.5.40)$$

To proceed further, it is necessary to express  $\theta|_{\xi=1}$  in terms of  $\theta_b$ . Hermite expansion for  $\alpha = 0, \beta = 0$ , Eq. (B) in Table 2.2, gives

$$\int_0^1 \theta (\xi - \xi^2) d\xi = \frac{\theta_b}{6} = \frac{1}{4} \frac{\partial [\theta (\xi - \xi^2)]}{\partial \xi} \Big|_{\xi=1} + \frac{1}{4} \frac{\partial [\theta (\xi - \xi^2)]}{\partial \xi} \Big|_{\xi=0} \quad (3.5.41)$$

On the other hand, Hermite expansion for  $\alpha = 1, \beta = 1$ , Eq. (B) in Table 2.5, yields

$$\begin{aligned} \int_0^1 \theta (\xi - \xi^2) d\xi = \frac{\theta_b}{6} = & \frac{1}{3} \theta (\xi - \xi^2)_{\xi=0} + \frac{2}{3} \theta (\xi - \xi^2)_{\xi=1} - \frac{1}{6} \frac{\partial [\theta (\xi - \xi^2)]}{\partial \xi} \Big|_{\xi=1} \\ & + \frac{1}{72} \left\{ \frac{\partial^2 [\theta (\xi - \xi^2)]}{\partial \xi^2} \Big|_{\xi=1} - \frac{\partial^2 [\theta (\xi - \xi^2)]}{\partial \xi^2} \Big|_{\xi=0} \right\} \end{aligned} \quad (3.5.42)$$

Substitution of the boundary conditions defined by Eqs. (3.5.10) and (3.5.11) into Eqs. (3.5.41) and (3.5.42) and the simultaneous solution of the resulting equations yield

$$\theta|_{\xi=1} = \left[ \frac{16}{3(6 + \Lambda)} \right] \theta_b \quad (3.5.43)$$

The use of Eq. (3.5.43) in Eq. (3.5.40) yields

$$\frac{d\theta_b}{d\eta} + \left( \frac{32\Lambda}{6 + \Lambda} \right) \theta_b = 0 \quad (3.5.44)$$

which is subject to the following boundary condition

$$\text{at } \eta = 0 \quad \theta_b = 1 \quad (3.5.45)$$

The solution of Eq. (3.5.44) is given by

$$\theta_{b,approx} = \exp \left[ - \left( \frac{32 \Lambda}{6 + \Lambda} \right) \eta \right] \quad (3.5.46)$$

### 3.5.3. Comparison of Results

A comparison of the analytical solution, Eq. (3.5.37), with the approximate one, Eq. (3.5.46), is presented in Figure 3.21 for various values of the Thiele modulus,  $\Lambda$ , which represents the ratio of the rate of surface reaction to the rate of diffusion. Numerical values are given in Table A.10 in Appendix A. In the calculation of  $\theta_b$  using Eq. (3.5.37), integration is performed numerically by MATHEMATICA<sup>®</sup>. Convergence is obtained by considering the first three terms of the series.

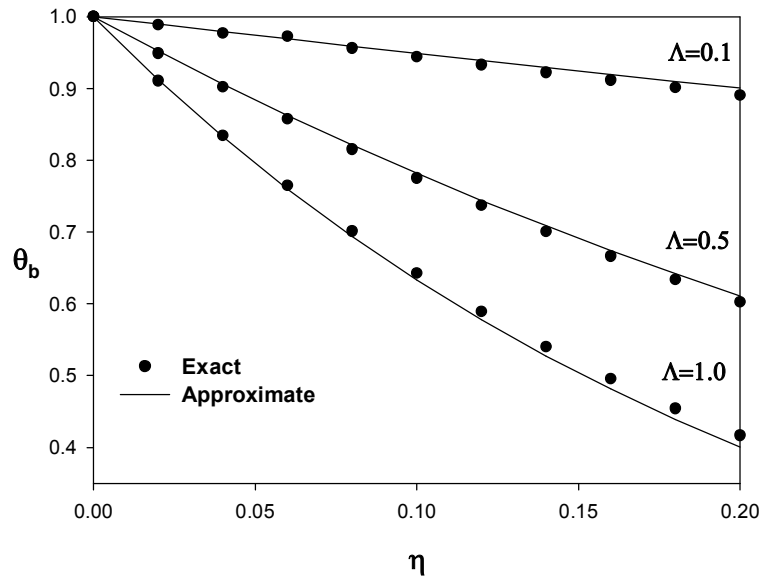


Figure 3.21. Comparison of the analytical and approximate solutions with  $\Lambda$  as a parameter.



The exact and approximate results are almost identical, the largest deviation being around 4% when  $\Lambda = 1.0$  and  $\eta = 0.2$ . As the Thiele modulus increases, the rate of surface reaction becomes more dominant than the rate of diffusion. As a result, species are consumed faster with a concomitant decrease in the bulk concentration,  $\theta_b$ .

### 3.6. Convective Mass Transport with a Wall Reaction in a Cylindrical Tube

In this section, the problem analyzed in the previous section is solved in cylindrical coordinate system. An incompressible Newtonian fluid flows in a cylindrical tube with a radius of  $R$  under the action of constant pressure gradient as shown in Figure 3.22. A first-order irreversible chemical reaction takes place on the wall of the cylinder. The system is isothermal and it is continuously fed at  $z = 0$  with a dilute solution of chemical reactant with a uniform concentration  $c_o$ . It is required to determine bulk concentration as a function of the axial direction under steady conditions.

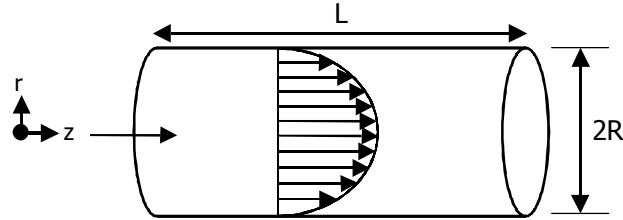


Figure 3.22. Convective mass transport in a cylindrical tube.

The fully-developed velocity profile is given by

$$v_z = \frac{(\mathcal{P}_o - \mathcal{P}_L) R^2}{4\mu L} \left[ 1 - \left( \frac{r}{R} \right)^2 \right] \quad (3.6.1)$$

For large values of Peclet number, the conservation of chemical species takes the form

$$\frac{(\mathcal{P}_o - \mathcal{P}_L) R^2}{4\mu L} \left[ 1 - \left( \frac{r}{R} \right)^2 \right] \frac{\partial c}{\partial z} = \frac{\mathcal{D}}{r} \frac{\partial}{\partial r} \left( r \frac{\partial c}{\partial r} \right) \quad (3.6.2)$$

The boundary conditions associated with Eq. (3.6.2) are

$$\text{at } z = 0 \quad c = c_o \quad (3.6.3)$$

$$\text{at } r = 0 \quad \frac{\partial c}{\partial r} = 0 \quad (3.6.4)$$

$$\text{at } r = R \quad -\mathcal{D} \frac{\partial c}{\partial r} = k'' c \quad (3.6.5)$$

Introduction of the following dimensionless variables

$$\theta = \frac{c}{c_o} \quad \xi = \frac{r}{R} \quad \eta = \frac{4\mu L \mathcal{D} z}{(\mathcal{P}_o - \mathcal{P}_L) R^4} \quad \Lambda = \frac{k'' R}{\mathcal{D}} \quad (3.6.6)$$

reduces Eqs. (3.6.2) – (3.6.5) to the form

$$(1 - \xi^2) \frac{\partial \theta}{\partial \eta} = \frac{1}{\xi} \frac{\partial}{\partial \xi} \left( \xi \frac{\partial \theta}{\partial \xi} \right) \quad (3.6.7)$$

$$\text{at } \eta = 0 \quad \theta = 1 \quad (3.6.8)$$

$$\text{at } \xi = 0 \quad \frac{\partial \theta}{\partial \xi} = 0 \quad (3.6.9)$$

$$\text{at } \xi = 1 \quad -\frac{\partial \theta}{\partial \xi} = \Lambda \theta \quad (3.6.10)$$

### 3.6.1. Analytical Solution

The method of separation of variables is employed in order to solve Eq. (3.6.7). The solution is written in product form as

$$\theta(\xi, \eta) = F(\xi) G(\eta) \quad (3.6.11)$$

so that Eq. (3.6.7) is split into two ordinary differential equations which are

$$\frac{dG}{d\eta} + \lambda_n^2 G = 0 \quad (3.6.12)$$

and

$$\frac{1}{\xi(1 - \xi^2)} \frac{d}{d\xi} \left( \xi \frac{dF}{d\xi} \right) + \lambda_n^2 F = 0 \quad (3.6.13)$$

The solution of Eq.(3.6.12) is

$$G_n(\eta) = \exp(-\lambda_n^2 \eta) \quad (3.6.14)$$

The use of the following transformations

$$X = \lambda_n \xi^2 \quad (3.6.15)$$

$$W_n(X) = \exp\left(\frac{X}{2}\right) F_n \quad (3.6.16)$$

reduces Eq. (3.6.13) to

$$X \frac{d^2 W_n}{dX^2} + (1 - X) \frac{dW_n}{dX} - \left(\frac{2 - \lambda_n}{4}\right) W_n = 0 \quad (3.6.17)$$

Comparison of Eq. (3.6.17) with Eq. (3.5.19) reveals that Eq. (3.6.17) is the Kummer's equation. The general solution of Eq. (3.6.17) is given by

$$W_n(X) = C_1 M\left(\frac{2 - \lambda_n}{4}, 1, X\right) + C_2 U\left(\frac{2 - \lambda_n}{4}, 1, X\right) \quad (3.6.18)$$

where  $M\left(\frac{2 - \lambda_n}{4}, 1, X\right)$  and  $U\left(\frac{2 - \lambda_n}{4}, 1, X\right)$  are Kummer's function of the first kind and second kind, respectively [8]. Equation (3.5.21) defines Kummer function of the first kind,  $M$ . Kummer function of the second kind,  $U$ , is defined by

$$U(a, b, x) = \frac{\Gamma(1 - b)}{\Gamma(a - b + 1)} M(a, b, x) + \frac{\Gamma(b - 1)}{\Gamma(a)} x^{1-b} M(a - b + 1, 2 - b, x) \quad (3.6.19)$$

where  $\Gamma(x)$  is the gamma function defined by

$$\Gamma(x) = \int_0^\infty t^{x-1} e^{-t} dt \quad (3.6.20)$$

Since  $U$  is unbounded when  $b = 1$ , i.e.,  $\Gamma(0) = \infty$ , the general solution becomes

$$W_n(X) = C_1 M\left(\frac{2 - \lambda_n}{4}, 1, X\right) \quad (3.6.21)$$

The boundary condition defined by Eq. (3.6.10) takes the form

$$\text{at } X = \lambda_n \quad -\frac{dW_n}{dX} = \left(\frac{\Lambda}{2\lambda_n} - \frac{1}{2}\right) W_n \quad (3.6.22)$$

The use of Eq. (3.6.22) gives the following transcendental equation for the eigenvalues  $\lambda_n$

$$\left(\frac{\Lambda}{\lambda_n} - 1\right) M\left(\frac{2-\lambda_n}{4}, 1, \lambda_n\right) = \left(\frac{2-\lambda_n}{2}\right) M\left(\frac{6-\lambda_n}{4}, 2, \lambda_n\right) \quad (3.6.23)$$

The first ten eigenvalues for various values of  $\Lambda$  are given in Table 3.9.

Table 3.9. The roots of Eq. (3.6.23) as a function of  $\Lambda$ .

$n$	$\Lambda = 0.1$	$\Lambda = 0.5$	$\Lambda = 1.0$	$\Lambda = 2.0$
1	0.6183	1.2716	1.6413	2.0000
2	5.1169	5.2951	5.4783	5.7439
3	9.1889	9.3063	9.4360	9.6451
4	13.2211	13.3119	13.4152	13.5903
5	17.2399	17.3153	17.4026	17.5548
6	21.2524	21.3177	21.3939	21.5295
7	25.2615	25.3194	25.3875	25.5105
8	29.2684	29.3207	29.3826	29.4955
9	33.2738	33.3217	33.3787	33.4834
10	37.2783	37.3225	37.3755	37.4733

The complete solution is given by

$$\theta(\xi, \eta) = \sum_{n=1}^{\infty} A_n F_n(\xi) \exp(-\lambda_n^2 \eta) \quad (3.6.24)$$

where

$$F_n(\xi) = \exp\left(-\frac{\lambda_n \xi^2}{2}\right) M\left(\frac{2-\lambda_n}{4}, 1, \lambda_n \xi^2\right) \quad (3.6.25)$$

The coefficients  $A_n$  are given as

$$A_n = \frac{\int_0^1 F_n(\xi) (1 - \xi^2) \xi d\xi}{\int_0^1 F_n^2(\xi) (1 - \xi^2) \xi d\xi} \quad (3.6.26)$$

The bulk concentration,  $c_b$ , is defined by

$$c_b = \frac{\int_0^{2\pi} \int_0^R cv_z r dr d\theta}{\int_0^{2\pi} \int_0^R v_z r dr d\theta} \quad (3.6.27)$$

In terms of the dimensionless quantities, Eq. (3.6.27) takes the form

$$\theta_b = \frac{c_b}{c_o} = \frac{\int_0^1 \theta (1 - \xi^2) \xi d\xi}{\int_0^1 (1 - \xi^2) \xi d\xi} = 4 \int_0^1 \theta (1 - \xi^2) \xi d\xi \quad (3.6.28)$$

Substitution of Eq. (3.6.24) into Eq. (3.6.28) and integration give the dimensionless bulk concentration as

$$\theta_{b,exact} = 4 \sum_{n=1}^{\infty} A_n \exp(-\lambda_n^2 \eta) \int_0^1 F_n(\xi) (1 - \xi^2) \xi d\xi \quad (3.6.29)$$

### 3.6.2. Approximate Solution by Area Averaging

Area averaging is performed by integrating Eq. (3.6.7) over the cross-sectional area of the system. For this purpose Eq. (3.6.7) is multiplied by  $\xi d\xi$  and integrated from  $\xi = 0$  to  $\xi = 1$ . The result is

$$\int_0^1 \xi (1 - \xi^2) \frac{\partial \theta}{\partial \eta} d\xi = \int_0^1 \frac{\partial}{\partial \xi} \left( \xi \frac{\partial \theta}{\partial \xi} \right) d\xi \quad (3.6.30)$$

or,

$$\frac{d}{d\eta} \int_0^1 \theta \xi (1 - \xi^2) d\xi = \xi \frac{\partial \theta}{\partial \xi} \Big|_{\xi=1} - \xi \frac{\partial \theta}{\partial \xi} \Big|_{\xi=0} \quad (3.6.31)$$

Substitution of Eq. (3.6.28) into the left-hand side, and the boundary conditions defined by Eqs. (3.6.9) and (3.6.10) into the right-hand side of Eq. (3.6.31) give

$$\frac{1}{4} \frac{d\theta_b}{d\eta} = -\Lambda \theta|_{\xi=1} \quad (3.6.32)$$

To proceed further, it is necessary to express  $\theta|_{\xi=1}$  in terms of  $\theta_b$ . Hermite expansion for  $\alpha = 0$  and  $\beta = 1$ , Eq. (A) in Table 2.4, gives

$$\int_0^1 \theta \xi (1 - \xi^2) d\xi = \frac{\theta_b}{4} = \frac{1}{3} (\theta \xi)|_{\xi=0} + \frac{2}{3} (\theta \xi)|_{\xi=1} - \frac{1}{6} \frac{\partial [\theta (1 - \xi^2) \xi]}{\partial \xi} \Big|_{\xi=1} \quad (3.6.33)$$

Substitution of the boundary conditions defined by Eqs. (3.6.9) and (3.6.10) into Eq. (3.6.33) results in

$$\theta|_{\xi=1} = \frac{3}{4} \theta_b \quad (3.6.34)$$

The use of Eq. (3.6.34) in Eq. (3.6.32) yields

$$\frac{d\theta_b}{d\eta} + 3\Lambda\theta_b = 0 \quad (3.6.35)$$

which is subject to the following boundary condition

$$\text{at } \eta = 0 \quad \theta_b = 1 \quad (3.6.36)$$

The solution of Eq. (3.6.35) is given by

$$\theta_{b,approx} = \exp(-3\Lambda\eta) \quad (3.6.37)$$

### 3.6.3. Comparison of Results

A comparison of the analytical solution, Eq. (3.6.29), with the approximate one, Eq. (3.6.37), is presented in Figure 3.23 for various values of the Thiele modulus,  $\Lambda$ , which represents the ratio of the rate of surface reaction to the rate of diffusion. Numerical values are given in Table A.11 in Appendix A. In the calculation of  $\theta_b$  using Eq. (3.6.29), integration is performed numerically using MATHEMATICA<sup>®</sup>. Convergence is obtained by considering the first three terms when  $\tau < 0.08$ . For larger values of  $\tau$ , the first two terms of the series are sufficient.

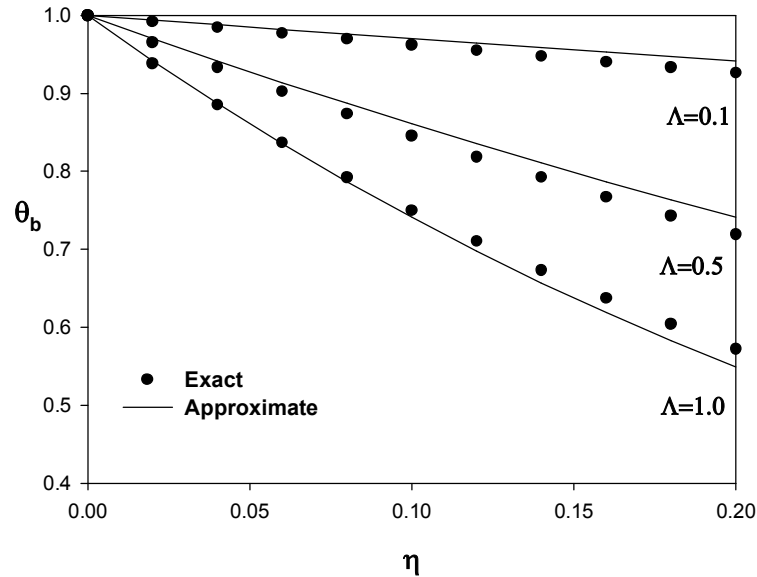


Figure 3.23. Comparison of the analytical and approximate solutions with  $\Lambda$  as a parameter.

The approximate solution gives fairly good estimates of the exact values in all cases considered. Approximate solution overestimates the analytical solution when  $\Lambda$  takes the values of 0.1 and 0.5. On the other hand, when  $\Lambda$  is increased to 1.0, the approximate method underestimates the analytical solution, the largest deviation being 3.7% when  $\Lambda = 1.0$  and  $\eta = 0.2$ . As the Thiele modulus increases, the rate of surface reaction becomes more dominant than the rate of diffusion. As a result, species are consumed faster with a concomitant decrease in the bulk concentration,  $\theta_b$ .

### 3.7. Unsteady Conduction in a Two-Layer Composite Slab

A composite plane wall, composed of two different layers of thicknesses  $L_1$  and  $L_2$ , is initially at a uniform temperature of  $T_o$ . The schematic representation of the system is shown in Figure 3.24. At  $t = 0$ , the surfaces at  $z = -L_1$  and  $z = L_2$  are exposed to fluids at temperature  $T_\infty$  ( $T_o < T_\infty$ ). The average heat transfer coefficients between the surfaces and the fluids are different from each other. It is required to find the variation of average temperatures within each slab with time as a result of unequal cooling conditions.

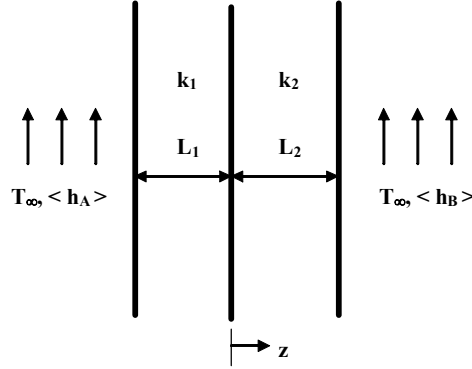


Figure 3.24. Conduction in a two-layer composite slab.

For a one-dimensional unsteady-state conduction, the equation of energy for each layer is given by

$$\frac{\partial T_i}{\partial t} = \alpha_i \frac{\partial^2 T_i}{\partial z^2} \quad i = 1, 2 \quad (3.7.1)$$

with the following initial and boundary conditions

$$\text{at } t = 0 \quad T_1 = T_2 = T_o \quad (3.7.2)$$

$$\text{at } z = -L_1 \quad -k_1 \frac{\partial T_1}{\partial z} = \langle h_A \rangle (T_\infty - T_1) \quad (3.7.3)$$

$$\text{at } z = 0 \quad T_1 = T_2 \quad (3.7.4)$$

$$\text{at } z = 0 \quad k_1 \frac{\partial T_1}{\partial z} = k_2 \frac{\partial T_2}{\partial z} \quad (3.7.5)$$

$$\text{at } z = L_2 \quad k_2 \frac{\partial T_2}{\partial z} = \langle h_B \rangle (T_\infty - T_2) \quad (3.7.6)$$

Introduction of the dimensionless variables

$$\theta = \frac{T_\infty - T_i}{T_\infty - T_o} \quad \xi = \frac{z}{L_1} \quad \tau = \frac{\alpha_1 t}{L_1^2} \quad \text{Bi}_A = \frac{\langle h_A \rangle L_1}{k_1} \quad \text{Bi}_B = \frac{\langle h_B \rangle L_2}{k_2}$$

$$\kappa = \frac{k_2}{k_1} \quad \gamma = \frac{L_2}{L_1} \quad \delta = \frac{\alpha_2}{\alpha_1} \quad (3.7.7)$$

reduces Eqs. (3.7.1) – (3.7.6) to the form

$$\frac{\partial \theta_1}{\partial \tau} = \frac{\partial^2 \theta_1}{\partial \xi^2} \quad (3.7.8)$$



$$\frac{\partial \theta_2}{\partial \tau} = \delta \frac{\partial^2 \theta_2}{\partial \xi^2} \quad (3.7.9)$$

$$\text{at } \tau = 0 \quad \theta_1 = \theta_2 = 1 \quad (3.7.10)$$

$$\text{at } \xi = -1 \quad \frac{\partial \theta_1}{\partial \xi} = \text{Bi}_A \theta_1 \quad (3.7.11)$$

$$\text{at } \xi = 0 \quad \theta_1 = \theta_2 \quad (3.7.12)$$

$$\text{at } \xi = 0 \quad \frac{\partial \theta_1}{\partial \xi} = \kappa \frac{\partial \theta_2}{\partial \xi} \quad (3.7.13)$$

$$\text{at } \xi = \gamma \quad -\frac{\partial \theta_2}{\partial \xi} = \frac{\text{Bi}_B}{\gamma} \theta_2 \quad (3.7.14)$$

### 3.7.1. Analytical Solution

The solution of this problem is given by Monte [9] as

$$\theta_1(\xi, \tau) = \sum_{n=1}^{\infty} A_n X_1(\xi) \exp(-\lambda_n^2 \tau) \quad (3.7.15)$$

$$\theta_2(\xi, \tau) = \frac{\sqrt{\delta}}{\kappa} \sum_{n=1}^{\infty} A_n X_2(\xi) \exp(-\lambda_n^2 \tau) \quad (3.7.16)$$

where

$$X_1(\xi) = \sin(\lambda_n \xi) + \Pi_1 \cos(\lambda_n \xi) \quad (3.7.17)$$

$$X_2(\xi) = \sin(\lambda_n \xi \sqrt{\delta}) - \Pi_2 \cos(\lambda_n \xi \sqrt{\delta}) \quad (3.7.18)$$

The eigenvalues,  $\lambda_n$ , are the roots of

$$\Pi_1 = -\frac{\sqrt{\delta}}{\kappa} \Pi_2 \quad (3.7.19)$$

where

$$\Pi_1 = \frac{\lambda_n + \text{Bi}_A \tan \lambda_n}{\text{Bi}_A - \lambda_n \tan \lambda_n} \quad (3.7.20)$$

$$\Pi_2 = \frac{u_n + (\text{Bi}_B / \kappa) \tan u_n}{(\text{Bi}_B / \kappa) - u_n \tan u_n} \quad (3.7.21)$$

$$u_n = \gamma \lambda_n / \sqrt{\delta} \quad (3.7.22)$$

The first ten eigenvalues for  $\gamma = 0.8$ ,  $\delta = 2.5$ , and different Biot numbers are tabulated in Table 3.10.

Table 3.10. The roots of Eq. (3.7.19) for  $\gamma = 0.8$ ,  $\delta = 2.5$ , and different Biot numbers.

$n$	$\text{Bi}_A = 0.5$	$\text{Bi}_A = 0.5$	$\text{Bi}_A = 1.0$	$\text{Bi}_A = 1.0$
	$\text{Bi}_B = 1.0$	$\text{Bi}_B = 5.0$	$\text{Bi}_B = 2.0$	$\text{Bi}_B = 5.0$
1	0.9263	1.2188	1.2027	1.3611
2	2.4048	2.8394	2.6695	2.9276
3	4.4494	4.7803	4.6293	4.8472
4	6.4195	6.7792	6.5715	6.8219
5	8.3938	8.6496	8.5022	8.6861
6	10.5893	10.7884	10.6759	10.8201
7	12.5932	12.8155	12.6759	12.8388
8	14.6063	14.7646	14.6701	14.7872
9	16.8164	16.9522	16.8723	16.9726
10	18.8195	18.9753	18.8756	18.9912

On the other hand, the coefficients  $A_n$  are given as

$$A_n = \frac{\kappa (\cos \lambda_n - \cos u_n + \Pi_1 \sin \lambda_n - \Pi_2 \sin u_n)}{N_n \lambda_n} \quad (3.7.23)$$

where

$$N_n = \frac{\kappa (1 + \Pi_1^2)}{2} \left( 1 + \frac{\text{Bi}_A}{\lambda_n^2 + \text{Bi}_A^2} \right) + \frac{\gamma (1 + \Pi_2^2)}{2} \left( 1 + \frac{\kappa \text{Bi}_B}{u_n^2 \kappa^2 + \text{Bi}_B^2} \right) \quad (3.7.24)$$

The average temperature,  $\langle T_i \rangle$ , for each layer is defined by

$$\langle T_1 \rangle = \frac{1}{L_1} \int_{-L_1}^0 T_1 dz \quad \langle T_2 \rangle = \frac{1}{L_2} \int_0^{L_2} T_2 dz \quad (3.7.25)$$

In terms of the dimensionless quantities, Eq. (3.7.25) takes the form

$$\langle \theta_1 \rangle = \frac{T_\infty - \langle T_1 \rangle}{T_\infty - T_o} = \int_{-1}^0 \theta_1 d\xi \quad (3.7.26)$$

$$\langle \theta_2 \rangle = \frac{T_\infty - \langle T_2 \rangle}{T_\infty - T_o} = \frac{1}{\gamma} \int_0^\gamma \theta_2 d\xi \quad (3.7.27)$$

Substitution of Eqs. (3.7.15) and (3.7.16) into Eqs. (3.7.26) and (3.7.27), respectively, and integration give

$$\langle \theta_1 \rangle_{exact} = \sum_{n=1}^{\infty} A_n \tilde{X}_1(\lambda_n) \exp(-\lambda_n^2 \tau) \quad (3.7.28)$$

$$\langle \theta_2 \rangle_{exact} = \frac{\sqrt{\delta}}{\kappa \gamma} \sum_{n=1}^{\infty} A_n \tilde{X}_2(\lambda_n) \exp(-\lambda_n^2 \tau) \quad (3.7.29)$$

where

$$\tilde{X}_1(\lambda_n) = \frac{1}{\lambda_n} (\cos \lambda_n + \Pi_1 \sin \lambda_n - 1) \quad (3.7.30)$$

$$\tilde{X}_2(\lambda_n) = \frac{\sqrt{\delta}}{\lambda_n} (1 - \cos u_n - \Pi_2 \sin u_n) \quad (3.7.31)$$

### 3.7.2. Approximate Solution by Area Averaging

Area averaging is performed by integrating Eqs. (3.7.8) and (3.7.9) in the direction of heat flow, i.e.,  $z$ -direction. For the first slab, Eq. (3.7.8) is multiplied by  $d\xi$  and integrated from  $\xi = -1$  to  $\xi = 0$ . The result is

$$\int_{-1}^0 \frac{\partial \theta_1}{\partial \tau} d\xi = \int_{-1}^0 \frac{\partial^2 \theta_1}{\partial \xi^2} d\xi \quad (3.7.32)$$

or,

$$\frac{d}{d\tau} \int_{-1}^0 \theta_1 d\xi = \left. \frac{\partial \theta_1}{\partial \xi} \right|_{\xi=0} - \left. \frac{\partial \theta_1}{\partial \xi} \right|_{\xi=-1} \quad (3.7.33)$$

Substitution of Eq. (3.7.28) into the left-hand side, and the boundary conditions defined by Eqs. (3.7.11) and (3.7.13) into the right-hand side of Eq. (3.7.33) give

$$\frac{d \langle \theta_1 \rangle}{d\tau} = \kappa \left. \frac{\partial \theta_2}{\partial \xi} \right|_{\xi=0} - \text{Bi}_A \theta_1|_{\xi=-1} \quad (3.7.34)$$

For the second slab, Eq. (3.7.9) is multiplied by  $d\xi$  and integrated from  $\xi = 0$  to  $\xi = \gamma$ . The result is

$$\int_0^\gamma \frac{\partial \theta_2}{\partial \tau} d\xi = \delta \int_0^\gamma \frac{\partial^2 \theta_2}{\partial \xi^2} d\xi \quad (3.7.35)$$

or,

$$\frac{d}{d\tau} \int_0^\gamma \theta_2 d\xi = \delta \left. \frac{\partial \theta_2}{\partial \xi} \right|_{\xi=\gamma} - \delta \left. \frac{\partial \theta_2}{\partial \xi} \right|_{\xi=0} \quad (3.7.36)$$

Substitution of Eq. (3.7.29) into the left-hand side, and the boundary conditions defined by Eq. (3.7.14) into the right-hand side of Eq. (3.7.36) give

$$\frac{d \langle \theta_2 \rangle}{d\tau} = -\frac{\delta}{\gamma^2} \text{Bi}_B \theta_2|_{\xi=\gamma} - \frac{\delta}{\gamma} \left. \frac{\partial \theta_2}{\partial \xi} \right|_{\xi=0} \quad (3.7.37)$$

To proceed further, it is necessary to express  $\theta_1|_{\xi=-1}$ ,  $\partial \theta_2 / \partial \xi|_{\xi=0}$ , and  $\theta_2|_{\xi=\gamma}$  in Eqs. (3.7.36) and (3.7.37) in terms of the average temperatures,  $\langle \theta_1 \rangle$  and  $\langle \theta_2 \rangle$ . Hermite expansion for  $\alpha = 1$ ,  $\beta = 0$ , Eq. (A) in Table 2.3, for  $\theta_1$  and  $\theta_2$  gives

$$\int_{-1}^0 \theta_1 d\xi = \langle \theta_1 \rangle = \frac{2}{3} \theta_1|_{\xi=-1} + \frac{1}{3} \theta_1|_{\xi=0} + \frac{1}{6} \left. \frac{\partial \theta_1}{\partial \xi} \right|_{\xi=-1} \quad (3.7.38)$$

$$\int_0^\gamma \theta_2 d\xi = \gamma \langle \theta_2 \rangle = \frac{2}{3} \theta_2|_{\xi=0} + \frac{1}{3} \theta_2|_{\xi=\gamma} + \frac{\gamma}{6} \left. \frac{\partial \theta_2}{\partial \xi} \right|_{\xi=0} \quad (3.7.39)$$

On the other hand, Hermite expansion for  $\alpha = 0$ ,  $\beta = 1$ , Eq. (A) in Table 2.4, for  $\theta_1$  and  $\theta_2$  yields

$$\int_{-1}^0 \theta_1 d\xi = \langle \theta_1 \rangle = \frac{1}{3} \theta_1|_{\xi=-1} + \frac{2}{3} \theta_1|_{\xi=0} - \frac{1}{6} \left. \frac{\partial \theta_1}{\partial \xi} \right|_{\xi=0} \quad (3.7.40)$$

$$\int_0^\gamma \theta_2 d\xi = \gamma \langle \theta_2 \rangle = \frac{1}{3} \theta_2|_{\xi=0} + \frac{2}{3} \theta_2|_{\xi=\gamma} - \frac{\gamma}{6} \left. \frac{\partial \theta_2}{\partial \xi} \right|_{\xi=\gamma} \quad (3.7.41)$$

Substitution of the corresponding boundary conditions defined by Eqs. (3.7.11)–(3.7.14) into Eqs. (3.7.38) – (3.7.41) gives

$$\langle \theta_1 \rangle = \left( \frac{4 + \text{Bi}_A}{6} \right) \theta_1|_{\xi=-1} + \frac{1}{3} \theta_1|_{\xi=0} \quad (3.7.42)$$

$$\langle \theta_1 \rangle = \frac{1}{3} \theta_1|_{\xi=-1} + \frac{2}{3} \theta_1|_{\xi=0} - \frac{\kappa}{6} \left. \frac{\partial \theta_2}{\partial \xi} \right|_{\xi=0} \quad (3.7.43)$$

$$\langle \theta_2 \rangle = \frac{2}{3\gamma} \theta_1|_{\xi=0} + \frac{1}{3\gamma} \theta_2|_{\xi=\gamma} + \frac{1}{6} \frac{\partial \theta_2}{\partial \xi} \Big|_{\xi=0} \quad (3.7.44)$$

$$\langle \theta_2 \rangle = \frac{1}{3\gamma} \theta_1|_{\xi=0} + \left( \frac{4 + \text{Bi}_B}{6\gamma} \right) \theta_2|_{\xi=\gamma} \quad (3.7.45)$$

Simultaneous solutions of Eqs. (3.7.42) – (3.7.45) give the relationships between average and local variables as

$$\theta_1|_{\xi=-1} = \frac{3 [2\kappa (3 + \text{Bi}_B) + \gamma (4 + \text{Bi}_B)]}{\varphi} \langle \theta_1 \rangle - \frac{3\kappa\gamma (2 + \text{Bi}_B)}{\varphi} \langle \theta_2 \rangle \quad (3.7.46)$$

$$\frac{\partial \theta_2}{\partial \xi} \Big|_{\xi=0} = -\frac{6(2 + \text{Bi}_A)(3 + \text{Bi}_B)}{\varphi} \langle \theta_1 \rangle + \frac{6\gamma(3 + \text{Bi}_A)(2 + \text{Bi}_B)}{\varphi} \langle \theta_2 \rangle \quad (3.7.47)$$

$$\theta_2|_{\xi=\gamma} = -\frac{3\gamma(2 + \text{Bi}_A)}{\varphi} \langle \theta_1 \rangle + \frac{3\gamma [\kappa(4 + \text{Bi}_A) + 2\gamma(3 + \text{Bi}_A)]}{\varphi} \langle \theta_2 \rangle \quad (3.7.48)$$

where

$$\varphi = \kappa(4 + \text{Bi}_A)(3 + \text{Bi}_B) + \gamma(3 + \text{Bi}_A)(4 + \text{Bi}_B) \quad (3.7.49)$$

Substitution of Eqs. (3.7.46) and (3.7.47) into Eq. (3.7.34) and substitution of Eqs. (3.7.47) and (3.7.48) into Eq. (3.7.37) result in

$$\frac{d \langle \theta_1 \rangle}{d\tau} = S_1 \langle \theta_1 \rangle + S_2 \langle \theta_2 \rangle \quad (3.7.50)$$

$$\frac{d \langle \theta_2 \rangle}{d\tau} = \frac{\delta}{\gamma^2 \kappa} S_2 \langle \theta_1 \rangle + S_3 \langle \theta_2 \rangle \quad (3.7.51)$$

where

$$S_1 = -\frac{3}{\varphi} [4\kappa(1 + \text{Bi}_A)(3 + \text{Bi}_B) + \gamma \text{Bi}_A(4 + \text{Bi}_B)] \quad (3.7.52)$$

$$S_2 = \frac{9\gamma\kappa(2 + \text{Bi}_A)(2 + \text{Bi}_B)}{\varphi} \quad (3.7.53)$$

$$S_3 = -\frac{3\delta}{\varphi} \left[ \frac{\text{Bi}_B}{\gamma} \kappa(4 + \text{Bi}_A) + 4(3 + \text{Bi}_A)(1 + \text{Bi}_B) \right] \quad (3.7.54)$$

The initial conditions associated with Eqs. (3.7.50) and (3.7.51) are

$$\text{at } \tau = 0 \quad \langle \theta_1 \rangle = \langle \theta_2 \rangle = 1 \quad (3.7.55)$$

Simultaneous solutions of Eqs. (3.7.50) and (3.7.51) by the Laplace transform give the average dimensionless temperature for each layer as

$$\langle \theta_1 \rangle_{approx} = \left[ \cosh(\Gamma\tau) + \left( \frac{S_1 + 2S_2 - S_3}{2} \right) \frac{\sinh(\Gamma\tau)}{\Gamma} \right] \exp \left[ \left( \frac{S_1 + S_3}{2} \right) \tau \right] \quad (3.7.56)$$

$$\langle \theta_2 \rangle_{approx} = \left[ \cosh(\Gamma\tau) + \left( S_3 - S_1 + \frac{\delta S_2}{\gamma^2 \kappa} \right) \frac{\sinh(\Gamma\tau)}{\Gamma} \right] \exp \left[ \left( \frac{S_1 + S_3}{2} \right) \tau \right] \quad (3.7.57)$$

where

$$\Gamma = \frac{\sqrt{4S_2^2\delta + \kappa\gamma^2(S_1 - S_3)^2}}{2\gamma\sqrt{\kappa}} \quad (3.7.58)$$

### 3.7.3. Comparison of Results

Comparisons of the analytical solutions, Eqs. (3.7.28) and (3.7.29) with the approximate ones, Eqs. (3.7.56) and (3.7.57), are presented in Figures 3.25–3.28 for  $\gamma = 0.8$ ,  $\delta = 2.5$  and different Biot numbers. Numerical values are given in Tables A.12–A.15 in Appendix A.

The terms  $\gamma$  and  $\delta$  represent thickness and thermal diffusivity ratios of the layers, respectively. In the calculations of  $\langle \theta_1 \rangle$  and  $\langle \theta_2 \rangle$  using Eqs. (3.7.28) and (3.7.29), the first seven terms of the series are used when  $\tau < 0.06$ . For larger  $\tau$  values, convergence is achieved by taking the first four terms.

The approximate solutions give good estimates of the analytical solutions for different Biot numbers. The approximate values slightly underestimate and overestimate the exact ones in the first and second layers, respectively, with the largest deviation being around 6%.

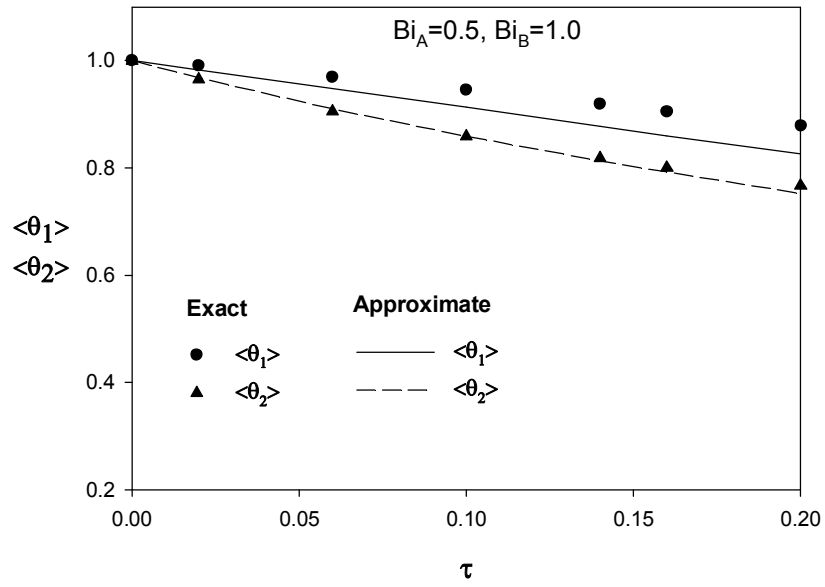


Figure 3.25. Comparison of the analytical and approximate solutions when  $Bi_A = 0.5$ ,  $Bi_B = 1.0$ .

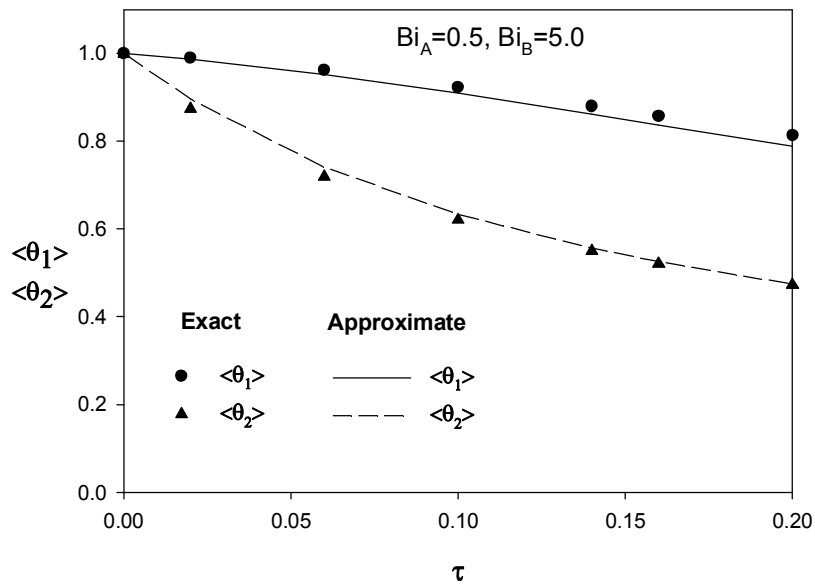


Figure 3.26. Comparison of the analytical and approximate solutions when  $Bi_A = 0.5$ ,  $Bi_B = 5.0$ .

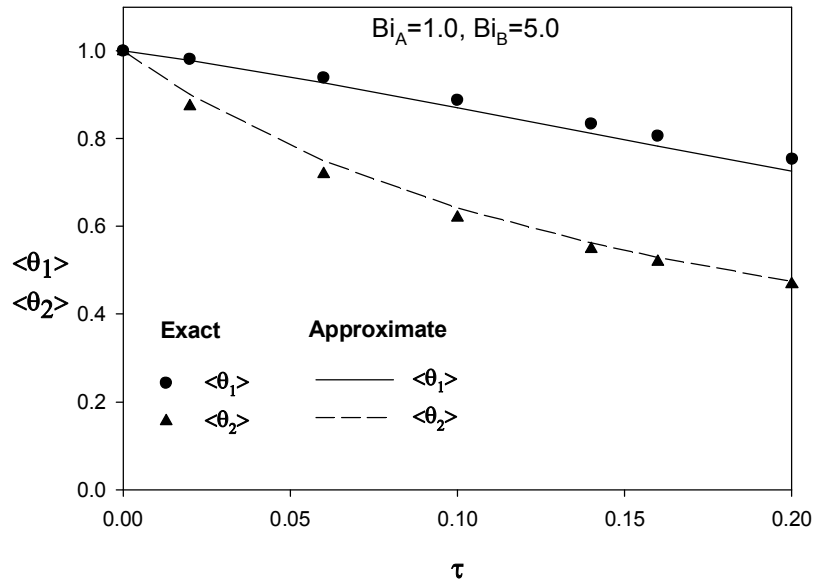


Figure 3.27. Comparison of the analytical and approximate solutions when  $Bi_A = 1.0, Bi_B = 5.0$ .

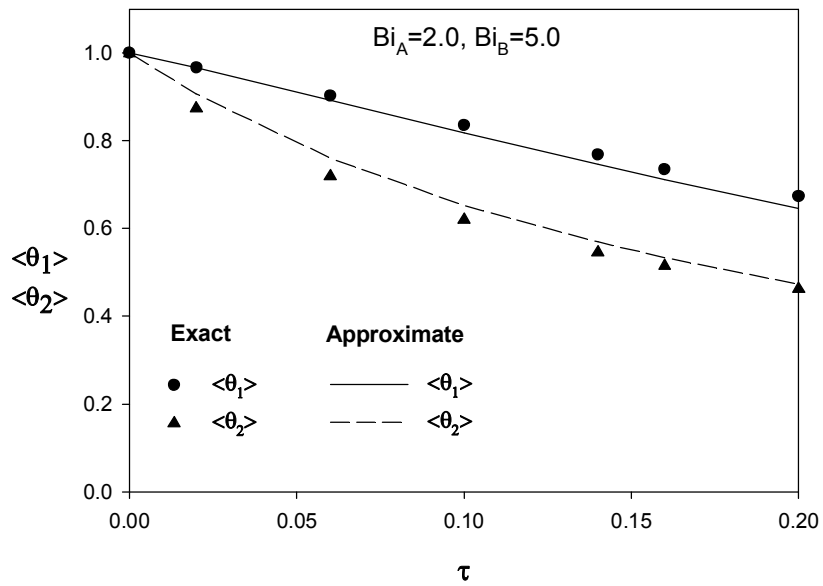


Figure 3.28. Comparison of the analytical and approximate solutions when  $Bi_A = 2.0, Bi_B = 5.0$ .



## CHAPTER 4

### CONCLUSIONS

In transport phenomena problems, obtaining an analytical solution is tedious if not impossible. In these cases, application of a numerical or an approximate technique is required. In this study, application of one of the approximate techniques, i.e., area averaging technique using the two-point Hermite expansion, is presented. By the application of the averaging procedure, the number of the independent variables in the partial differential equation defining the problems is reduced by one. This simplification of the problem however, requires expressing the local value of the dependent variable and/or its derivative(s) on the system boundaries in terms of the averaged variable. In this study, such a relationship is obtained by employing the two-point Hermite expansion.

Two-point Hermite expansion has two parameters,  $\alpha$  and  $\beta$ . There is no clear-cut recipe to pick the right  $\alpha$  and  $\beta$  values that will yield the best results. Depending on the governing equation and the boundary conditions, one of the methods to choose the appropriate  $\alpha$  and  $\beta$  values is to check whether the approximate solution converges to the analytical one under steady conditions. Obtaining identical expression for the steady-state case does not necessarily guarantee that the applied Hermite expansion is the best choice. However, the chances of obtaining good results are high. Even though the application of single  $\alpha = 0, \beta = 0$  Hermite expansion is simpler, it does not yield very satisfactory estimates of the exact values. Combination of two Hermite expansions, such as  $\alpha = 1, \beta = 0$  and  $\alpha = 0, \beta = 1$ , yields better results than  $\alpha = 0, \beta = 0$  Hermite expansion.

In the problems analyzed in this study, area averaging technique using Hermite expansion generally gives better estimates of the exact values for the smaller values of the independent variable, time or space, provided that the boundary conditions associated with the eliminated independent variable are used in the averaged equation.

In some problems, even if an analytical solution exists, calculation of eigenvalues and coefficients can be very tedious. In these cases, area averaging technique using Hermite expansion is useful. Moreover, this approximate method can also be utilized to obtain initial guesses for the numerical analysis. This decreases the computational effort and time for the convergence of the numerical techniques.

The problems analyzed in this study are unsteady flow in a concentric annulus, unequal cooling of a long slab, unsteady conduction in a cylindrical rod with internal heat generation, diffusion of a solute into a slab from limited volume of a well-mixed solution, convective mass transport between two parallel plates with a wall reaction, convective mass transport in a cylindrical tube with a wall reaction, and unsteady conduction in a two-layer composite slab.

In unsteady flow in a concentric annulus problem, the analytical and approximate solutions are compared for different values of radius ratio. The approximate results slightly overestimates the exact ones with the largest deviation being 13%.

In unequal cooling of a long slab problem, the analytical and approximate solutions are compared for different Biot numbers. Approximate results almost coincide with the exact ones, the largest deviation being approximately 8%.

In unsteady conduction in a cylindrical rod with internal heat generation problem, the analytical and approximate solutions are compared for different Biot numbers and the dimensionless generation term. The approximate solution gives satisfactory estimates of the analytical one for relatively small values of the Biot number. The deviation from the analytical solution increases as the values of the Biot number and the dimensionless generation term increase. The largest deviation is about 18%.

In diffusion of a solute into a slab from limited volume of a well-mixed solution problem, the analytical and approximate solutions are compared for various values of the ratio of the solution volume to the product of the slab volume and the partition coefficient. The exact and approximate results are almost identical except for the small values of dimensionless time. The largest deviation is about 27% only when  $\tau = 0.1$ .

In convective mass transport problems, either between two parallel plates, or in a cylindrical tube with a wall reaction, the analytical and approximate solutions are compared for different values of the Thiele modulus. The approximate solutions give fairly good estimates of the exact values, the largest deviations being around 4% in both of the cases.

In unsteady conduction in a two-layer composite slab problem, the analytical and approximate solutions are compared for different Biot numbers. The approximate values slightly underestimate and overestimate the exact ones in the first and second layers, respectively, with the largest deviation being around 6%.

## REFERENCES

- [1] Mennig, J., Auerbsch, T., Halg, W. (1983) Two Point Hermite Approximations for the Solution of Linear Initial Value and Boundary Value Problems. Computer Methods in Applied Mechanics and Engineering. Vol. 39, p. 199-224.
- [2] Özyılmaz, M., (1996) Solutions of Transport Phenomena Problems by Averaging Techniques. Master of Science Thesis. METU, Chemical Engineering.
- [3] Müller, W., Z. Angew. (1936) Zum Problem der Anlaufströmung einer Flüssigkeit imgeraden Rohr mit Kreisring-und Kreisquerschnitt. Math. Mech., Vol.16, p. 227-238.
- [4] Su, J. (2001) Improved lumped models for asymmetric cooling of a long slab by heat convection. Int. Comm. Heat Mass Transfer, Vol. 28, No. 7 p. 973-983.
- [5] Tosun, I. (2007) Modeling in Transport Phenomena, 2nd Ed., Elsevier, p. 518-519.
- [6] Carslaw, H. S., Jaeger, J. C. (1959) Conduction of Heat in Solids. Clarendon Press, Oxford, .
- [7] Tosun, I. (2007) Modeling in Transport Phenomena, 2nd Ed., Elsevier, p. 446.
- [8] Abramowitz, M., Stegun, I. (1974) Handbook of Mathematical Functions, Dover Publications, Inc., Newyork.
- [9] Monte, F. (2000) Transient heat conduction in one-dimensional composite slab. International Journal of Heat and Mass Transfer, Vol. 43, p. 3607-3619.

# APPENDIX

## NUMERICAL RESULTS OF THE SOLUTIONS

In this section, numerical results of the analytical and approximate solutions of the problems given in Chapter 3 are tabulated in Tables A.1–A.15.

Table A.1. Numerical results of Eqs. (3.1.28) and (3.1.39) with  $\kappa$  as a parameter.

$\kappa = 0.1$			$\kappa = 0.2$		
$\tau$	Exact	Hermite	$\tau$	Exact	Hermite
0.00	0.000	0.000	0.00	0.000	0.000
0.01	0.0330	0.0368	0.01	0.0312	0.0350
0.02	0.0609	0.0685	0.02	0.0565	0.0640
0.04	0.106	0.120	0.04	0.0963	0.108
0.06	0.142	0.157	0.06	0.126	0.138
0.08	0.171	0.186	0.08	0.148	0.159
0.10	0.194	0.207	0.10	0.164	0.173
0.12	0.212	0.222	0.12	0.177	0.183
0.14	0.227	0.234	0.14	0.186	0.190
0.16	0.239	0.242	0.16	0.193	0.195
0.18	0.248	0.249	0.18	0.198	0.198
0.20	0.256	0.253	0.20	0.202	0.200

Table A.2. Numerical results of Eqs. (3.1.28) and (3.1.39) with  $\kappa$  as a parameter.

$\kappa = 0.3$			$\kappa = 0.4$		
$\tau$	Exact	Hermite	$\tau$	Exact	Hermite
0.00	0.000	0.000	0.00	0.000	0.000
0.01	0.0286	0.0323	0.01	0.0253	0.0286
0.02	0.0508	0.0576	0.02	0.0435	0.0490
0.04	0.0835	0.0928	0.04	0.0679	0.0742
0.06	0.1057	0.1144	0.06	0.0821	0.0872
0.08	0.1206	0.1277	0.08	0.0900	0.0938
0.10	0.1307	0.1358	0.10	0.0950	0.0972
0.12	0.1376	0.1408	0.12	0.0980	0.0990
0.14	0.1423	0.1438	0.14	0.1000	0.0999
0.16	0.1454	0.1457	0.16	0.1010	0.1003
0.18	0.1476	0.1468	0.18	0.1010	0.1006
0.20	0.1490	0.1475	0.20	0.1020	0.1007

Table A.3. Numerical results of Eqs. (3.1.28) and (3.1.39) with  $\kappa$  as a parameter.

$\kappa = 0.5$			$\kappa = 0.6$		
$\tau$	Exact	Hermite	$\tau$	Exact	Hermite
0.00	0.000	0.000	0.00	0.000	0.000
0.01	0.0210	0.0238	0.01	0.0160	0.0180
0.02	0.0346	0.0386	0.02	0.0244	0.0265
0.04	0.0500	0.0533	0.04	0.0314	0.0324
0.06	0.0570	0.0590	0.06	0.0334	0.0338
0.08	0.0603	0.0612	0.08	0.0340	0.0340
0.10	0.0617	0.0620	0.10	0.0342	0.0341
0.12	0.0624	0.0623	0.12	0.0343	0.0341
0.14	0.0627	0.0624	0.14	0.0343	0.0341
0.16	0.0629	0.0625	0.16	0.0343	0.0341
0.18	0.0629	0.0625	0.18	0.0343	0.0341
0.20	0.0630	0.0625	0.20	0.0343	0.0341

Table A.4. Numerical results of Eqs. (3.1.28) and (3.1.39) with  $\kappa$  as a parameter.

$\kappa = 0.7$			$\kappa = 0.8$		
$\tau$	Exact	Hermite	$\tau$	Exact	Hermite
0.00	0.000	0.000	0.00	0.000	0.000
0.01	0.0102	0.0113	0.01	0.00440	0.00456
0.02	0.0136	0.0142	0.02	0.00477	0.00479
0.04	0.0151	0.0152	0.04	0.00480	0.00480
0.06	0.0153	0.0153	0.06	0.00480	0.00480
0.08	0.0153	0.0153	0.08	0.00480	0.00480
0.10	0.0153	0.0153	0.10	0.00480	0.00480
0.12	0.0153	0.0153	0.12	0.00480	0.00480
0.14	0.0153	0.0153	0.14	0.00480	0.00480
0.16	0.0153	0.0153	0.16	0.00480	0.00480
0.18	0.0153	0.0153	0.18	0.00480	0.00480
0.20	0.0153	0.0153	0.20	0.00480	0.00480

Table A.5. Numerical results of Eqs. (3.2.28) and (3.2.39) with Biot numbers as parameters .

$\text{Bi}_A = 1.0, \text{Bi}_B = 0.1$			$\text{Bi}_A = 5.0, \text{Bi}_B = 1.0$			$\text{Bi}_A = 10.0, \text{Bi}_B = 1.0$		
$\tau$	Exact	Hermite	$\tau$	Exact	Hermite	$\tau$	Exact	Hermite
0.00	1.000	1.000	0.00	1.000	1.000	0.00	1.000	1.000
0.01	0.9799	0.9804	0.01	0.9454	0.9582	0.01	0.9258	0.9518
0.10	0.8124	0.8120	0.10	0.6218	0.6371	0.10	0.5670	0.5919
0.20	0.6420	0.6396	0.20	0.3717	0.3742	0.20	0.3119	0.3134
0.30	0.4856	0.4817	0.30	0.1891	0.1836	0.30	0.1344	0.1232
0.50	0.2103	0.2044	0.50	-0.0437	-0.0546	0.50	-0.0778	-0.0952
0.70	-0.0213	-0.0286	0.70	-0.1697	-0.1798	0.70	-0.1828	-0.1969
1.00	-0.3018	-0.3099	1.00	-0.2591	-0.2655	1.00	-0.2499	-0.2575
1.25	-0.4859	-0.4942	1.25	-0.2907	-0.2946	1.25	-0.2708	-0.2748
1.50	-0.6343	-0.6424	1.50	-0.3054	-0.3076	1.50	-0.2795	-0.2815
2.00	-0.8502	-0.8572	2.00	-0.3154	-0.3161	2.00	-0.2847	-0.2851

Table A.6. Numerical results of Eqs. (3.3.26) and (3.3.34) for  $\text{Bi} = 0.1$  with  $\Lambda$  as a parameter.

Bi = 0.1, $\Lambda = 1.0$			Bi = 0.1, $\Lambda = 10.0$			Bi = 0.1, $\Lambda = 50.0$		
$\tau$	Exact	Hermite	$\tau$	Exact	Hermite	$\tau$	Exact	Hermite
0.00	1.000	1.000	0.00	1.000	1.000	0.00	1.000	1.000
0.02	1.006	1.009	0.02	1.096	1.099	0.02	1.494	1.499
0.04	1.012	1.019	0.04	1.191	1.199	0.04	1.985	1.996
0.06	1.018	1.029	0.06	1.286	1.298	0.06	2.480	2.490
0.08	1.024	1.038	0.08	1.380	1.396	0.08	2.961	2.983
0.10	1.030	1.048	0.10	1.474	1.493	0.10	3.445	3.474
0.12	1.036	1.056	0.12	1.567	1.590	0.12	3.928	3.962
0.14	1.042	1.065	0.14	1.659	1.687	0.14	4.410	4.448
0.16	1.048	1.073	0.16	1.752	1.783	0.16	4.886	4.933
0.18	1.054	1.082	0.18	1.845	1.878	0.18	5.355	5.415
0.20	1.062	1.090	0.20	1.937	1.973	0.20	5.836	5.895

Table A.7. Numerical results of Eqs. (3.3.26) and (3.3.34) for  $\text{Bi} = 1$  with  $\Lambda$  as a parameter.

Bi = 1, $\Lambda = 10$			Bi = 1, $\Lambda = 50$			Bi = 1, $\Lambda = 100$		
$\tau$	Exact	Hermite	$\tau$	Exact	Hermite	$\tau$	Exact	Hermite
0.00	1.000	1.000	0.00	1.000	1.000	0.00	1.000	1.000
0.02	1.061	1.098	0.02	1.449	1.491	0.02	1.934	1.982
0.04	1.120	1.191	0.04	1.876	1.964	0.04	2.819	2.930
0.06	1.177	1.279	0.06	2.282	2.419	0.06	3.665	3.845
0.08	1.232	1.363	0.08	2.674	2.858	0.08	4.477	4.727
0.10	1.285	1.442	0.10	3.050	3.280	0.10	5.258	5.578
0.12	1.336	1.518	0.12	3.413	3.687	0.12	6.010	6.399
0.14	1.385	1.589	0.14	3.764	4.079	0.14	6.737	7.190
0.16	1.433	1.657	0.16	4.101	4.455	0.16	7.438	7.954
0.18	1.479	1.720	0.18	4.428	4.818	0.18	8.116	8.690
0.20	1.524	1.780	0.20	4.750	5.167	0.20	8.772	9.400



Table A.8. Numerical results of Eqs. (3.3.26) and (3.3.34) for  $\text{Bi} = 5$  with  $\Lambda$  as a parameter.

Bi = 5, $\Lambda = 50$			Bi = 5, $\Lambda = 100$			Bi = 5, $\Lambda = 300$		
$\tau$	Exact	Hermite	$\tau$	Exact	Hermite	$\tau$	Exact	Hermite
0.00	1.000	1.000	0.00	1.000	1.000	0.00	1.000	1.000
0.02	1.315	1.472	0.02	1.758	1.945	0.02	3.526	3.839
0.04	1.596	1.889	0.04	2.405	2.788	0.04	5.642	6.382
0.06	1.842	2.260	0.06	2.972	3.539	0.06	7.486	8.656
0.08	2.070	2.586	0.08	3.476	4.207	0.08	9.122	10.690
0.10	2.265	2.873	0.10	3.931	4.800	0.10	10.593	12.509
0.12	2.445	3.126	0.12	4.341	5.327	0.12	11.925	14.133
0.14	2.611	3.346	0.14	4.718	5.794	0.14	13.140	15.585
0.16	2.764	3.538	0.16	5.062	6.206	0.16	14.252	16.880
0.18	2.903	3.704	0.18	5.377	6.570	0.18	15.273	18.036
0.20	3.032	3.848	0.20	5.668	6.891	0.20	16.211	19.066

Table A.9. Numerical results of Eqs. (3.4.18) and (3.4.32) with  $\Psi$  as a parameter.

$\Psi = 50.0$			$\Psi = 10.0$			$\Psi = 1.0$		
$\tau$	Exact	Hermite	$\tau$	Exact	Hermite	$\tau$	Exact	Hermite
0.00	0.00	0.00	0.00	0.00	0.00	0.00	0.00	0.00
0.10	0.3619	0.2636	0.10	0.3818	0.2811	0.10	0.5528	0.4512
0.20	0.5101	0.4577	0.20	0.5332	0.4831	0.20	0.7116	0.6988
0.30	0.6195	0.6007	0.30	0.6431	0.6284	0.30	0.8096	0.8347
0.40	0.7039	0.7059	0.40	0.7266	0.7329	0.40	0.8739	0.9093
0.50	0.7696	0.7835	0.50	0.7906	0.8080	0.50	0.9165	0.9502
0.60	0.8207	0.8405	0.60	0.8395	0.8619	0.60	0.9447	0.9727
0.80	0.8914	0.9135	0.80	0.9058	0.9286	0.80	0.9757	0.9918
0.10	0.9342	0.9531	0.10	0.9447	0.9631	0.10	0.9893	0.9975
0.12	0.9602	0.9746	0.12	0.9675	0.9809	0.12	0.9953	0.9993

Table A.10. Numerical results of Eqs. (3.5.37) and (3.5.46) with  $\Lambda$  as a parameter.

$\Lambda = 0.1$			$\Lambda = 0.5$			$\Lambda = 1.0$		
$\tau$	Exact	Hermite	$\tau$	Exact	Hermite	$\tau$	Exact	Hermite
0.00	1.000	1.000	0.00	1.000	1.000	0.00	1.000	1.000
0.02	0.9884	0.9896	0.02	0.9487	0.9520	0.02	0.9106	0.9126
0.04	0.9770	0.9792	0.04	0.9018	0.9062	0.04	0.8341	0.8329
0.06	0.9725	0.9690	0.06	0.8573	0.8627	0.06	0.7646	0.7601
0.08	0.9560	0.9589	0.08	0.8151	0.8213	0.08	0.7010	0.6937
0.10	0.9437	0.9489	0.10	0.7750	0.7818	0.10	0.6427	0.6331
0.12	0.9328	0.9390	0.12	0.7368	0.7442	0.12	0.5892	0.5778
0.14	0.9221	0.9292	0.14	0.7005	0.7085	0.14	0.5402	0.5273
0.16	0.9115	0.9195	0.16	0.6661	0.6745	0.16	0.4953	0.4812
0.18	0.9010	0.9099	0.18	0.6333	0.6421	0.18	0.4541	0.4392
0.20	0.8906	0.9004	0.20	0.6021	0.6112	0.20	0.4163	0.4008

Table A.11. Numerical results of Eqs. (3.6.29) and (3.6.37) with  $\Lambda$  as a parameter.

$\Lambda = 0.1$			$\Lambda = 0.5$			$\Lambda = 1.0$		
$\tau$	Exact	Hermite	$\tau$	Exact	Hermite	$\tau$	Exact	Hermite
0.00	1.000	1.000	0.00	1.000	1.000	0.00	1.000	1.000
0.02	0.9921	0.9940	0.02	0.9651	0.9704	0.02	0.9380	0.9418
0.04	0.9846	0.9880	0.04	0.9331	0.9418	0.04	0.8852	0.8869
0.06	0.9771	0.9822	0.06	0.9026	0.9139	0.06	0.8368	0.8353
0.08	0.9696	0.9763	0.08	0.8735	0.8869	0.08	0.7919	0.7866
0.10	0.9622	0.9704	0.10	0.8454	0.8607	0.10	0.7498	0.7408
0.12	0.9548	0.9646	0.12	0.8184	0.8353	0.12	0.7101	0.6977
0.14	0.9476	0.9589	0.14	0.7923	0.8106	0.14	0.6727	0.6570
0.16	0.9403	0.9531	0.16	0.7671	0.7866	0.16	0.6373	0.6188
0.18	0.9332	0.9474	0.18	0.7426	0.7633	0.18	0.6039	0.5827
0.20	0.9261	0.9418	0.20	0.7190	0.7408	0.20	0.5721	0.5488

Table A.12. Numerical results of Eqs. (3.7.28) – (3.7.56) and (3.7.29) – (3.7.57) when  $\text{Bi}_1=0.5$   $\text{Bi}_2=1.0$ .

$\text{Bi}_1=0.5$ $\text{Bi}_2=1.0$	Exact		Hermite	
$\tau$	$\langle\theta_1\rangle$	$\langle\theta_2\rangle$	$\langle\theta_1\rangle$	$\langle\theta_2\rangle$
0	1.0000	1.0000	1.0000	1.0000
0.02	0.9905	0.9648	0.9830	0.9678
0.06	0.9696	0.9058	0.9481	0.9098
0.10	0.9451	0.8586	0.9129	0.8587
0.14	0.9188	0.8186	0.8776	0.8131
0.16	0.9054	0.8005	0.8602	0.7919
0.20	0.8782	0.7669	0.8257	0.7524

Table A.13. Numerical results of Eqs. (3.7.28) – (3.7.56) and (3.7.29) – (3.7.57) when  $\text{Bi}_1=0.5$   $\text{Bi}_2=5.0$ .

$\text{Bi}_1=0.5$ $\text{Bi}_2=5.0$	Exact		Hermite	
$\tau$	$\langle\theta_1\rangle$	$\langle\theta_2\rangle$	$\langle\theta_1\rangle$	$\langle\theta_2\rangle$
0	1.0000	1.0000	1.0000	1.0000
0.02	0.9903	0.8743	0.9879	0.8959
0.06	0.9623	0.7192	0.9528	0.7406
0.10	0.9232	0.6208	0.9092	0.6333
0.14	0.8797	0.5502	0.8618	0.5561
0.16	0.8574	0.5214	0.8375	0.5252
0.20	0.8131	0.4726	0.7892	0.4741

Table A.14. Numerical results of Eqs. (3.7.28) – (3.7.56) and (3.7.29) – (3.7.57) when  $\text{Bi}_1=1.0$   $\text{Bi}_2=5.0$ .

$\text{Bi}_1=1.0$ $\text{Bi}_2=5.0$	Exact		Hermite	
$\tau$	$\langle\theta_1\rangle$	$\langle\theta_2\rangle$	$\langle\theta_1\rangle$	$\langle\theta_2\rangle$
0	1.0000	1.0000	1.0000	1.0000
0.02	0.9817	0.8742	0.9789	0.9002
0.06	0.9393	0.7191	0.9278	0.7490
0.10	0.8876	0.6203	0.8707	0.6417
0.14	0.8334	0.5487	0.8119	0.5621
0.16	0.8063	0.5191	0.7828	0.5295
0.20	0.7534	0.4683	0.7260	0.4743

Table A.15. Numerical results of Eqs. (3.7.28) – (3.7.56) and (3.7.29) – (3.7.57) when  $Bi_1=2.0$   $Bi_2=5.0$ .

$Bi_1=2.0$ $Bi_2=5.0$	Exact		Hermite	
$\tau$	$\langle\theta_1\rangle$	$\langle\theta_2\rangle$	$\langle\theta_1\rangle$	$\langle\theta_2\rangle$
0	1.0000	1.0000	1.0000	1.0000
0.02	0.9669	0.8742	0.9659	0.9064
0.06	0.9030	0.7191	0.8928	0.7606
0.10	0.8349	0.6197	0.8183	0.6527
0.14	0.7676	0.5464	0.7461	0.5692
0.16	0.7351	0.5156	0.7114	0.5340
0.20	0.6732	0.4618	0.6456	0.4731